Chapter 1

General Introduction and Review of Literature

1.1 Introduction

Throughout the recent decades it has been established that conventionally used organic solvents such as halogenated hydrocarbons, n-hexane, tetrachloroethylene, benzene, toluene etc. pose crucial environmental and human health concerns which include atmospheric emissions, contamination of water bodies, carcinogenic nature, reproductive hazards, neurotoxic nature etc. From this perspective, ionic liquids have emerged as a promising environmentally benign alternative to the volatile organic solvents [1, 2].

Ionic liquids comprise an extremely broad class of organic salts and possess wide temperature windows to remain in liquid state. The term "room temperature ionic liquids" (RTILs) is used to represent organic salts which are liquid at room temperature [3,4]. Ionic liquids (ILs) are also known by several different names like neoteric solvents, designer solvents, ionic fluids, and molten salts [2]. The main advantages of ILs are that their physicochemical properties like polarity, melting points, hydrophobicity, density, ionic conductivity, viscosity, thermal stability, water sensitivity, electrochemical stability, ability to dissolve different solutes as well as miscibility with varied nature of solvents can be tuned by making suitable combinations of organic cations and organic/inorganic anions or through tethering of functionalized side chains to the ions [5]. This has earned them the accolade of 'designer solvents' and it is often utilized to design and synthesize ILs for specific uses known as 'task-specific ionic liquids' (TSILs). In the recent past, ILs have been perceived as a class of prospective material with unique physicochemical properties that originate from their significantly wide range of the cation-anion pair combinations at room temperature, their inherent binary nature, the coexistence of distinct local molecular environments that can be controlled through substitution, their complex transport properties, and many other intriguing properties [6].

Some of the commonly used organic cations in the ILs are imidazolium, ammonium, pyridinium and phosphonium cations and they are often combined with different inorganic (Cl^-, BF_4^-, PF_6^-, Br^-, OH^-, NO_3^- etc.) and organic (CH_3COO^-, CF_3COO^-, Tf_2N^-, OTf^- etc.) anions **(Fig. 1.1)**.

Generally, the ILs are neutral or weakly basic in nature in the presence of distinct anions like BF_4^-, SCN^-, p-toluene sulfonate, NTf_2^- etc. Basic IL-forming anions include hydroxide, lactate, formate, carboxylate, dicyanamide, etc.

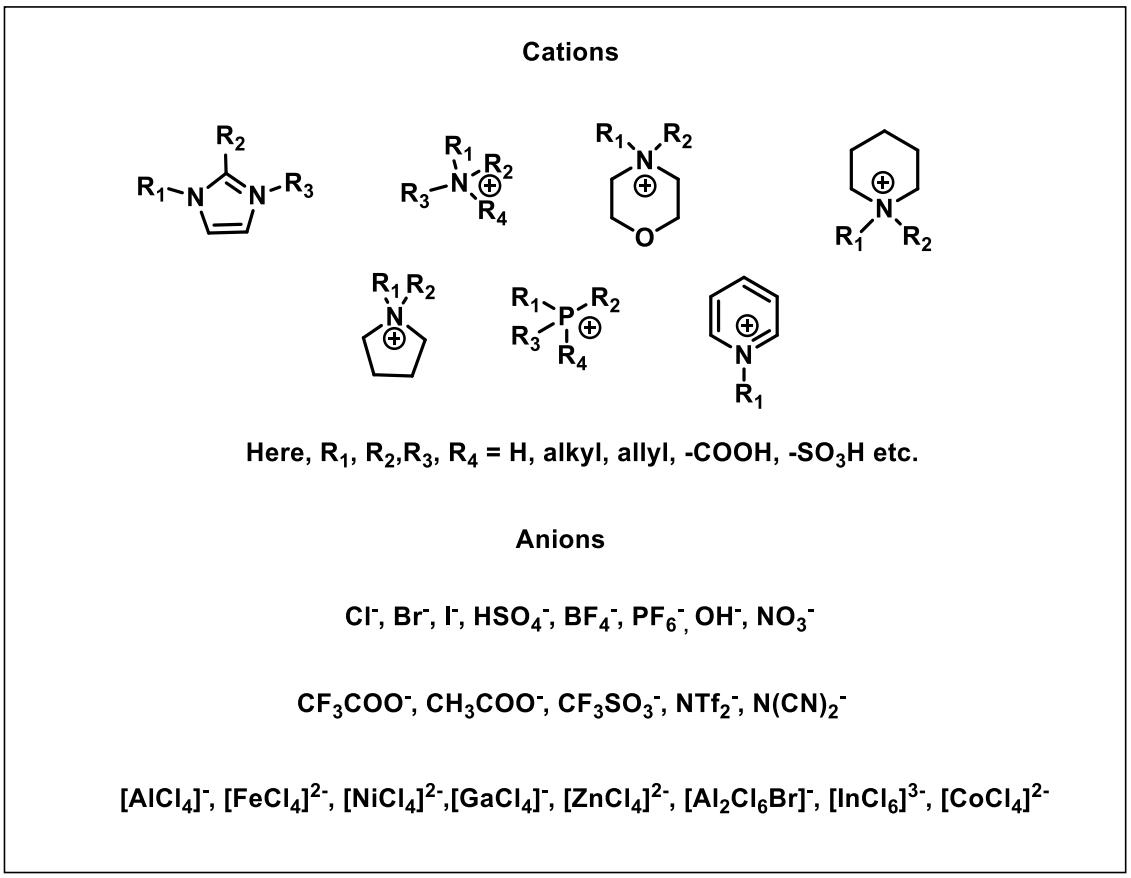

Fig. 1.1: Commonly used cations and anions in ionic liquids.

If the acidic or basic functional groups are tethered to the constituent ions, then they start behaving as task-specific acidic or basic ILs. The acidity of the ILs can be Brønsted, Lewis or both Brønsted-Lewis acidic depending on the type of acidic sites present. Apart from these, few amphoteric ILs are also known whose anions bear the capacity to both accept and donate protons (for example: bisulfate, dialkyl phosphate, etc.) based on the type of substrates present [7]. **Fig 1.2** shows various classifications of the ILs. In recent years, the tuning of physicochemical properties of ILs have made them fascinating and advantageous materials for potential applications in different fields like catalysis [7-11], analytical chemistry [12, 13], biomass conversion [14, 15], nanotechnology [16-18], sensors [19, 20], energy conversion device [21, 22], polymer science [23], pharmaceuticals [24] etc.

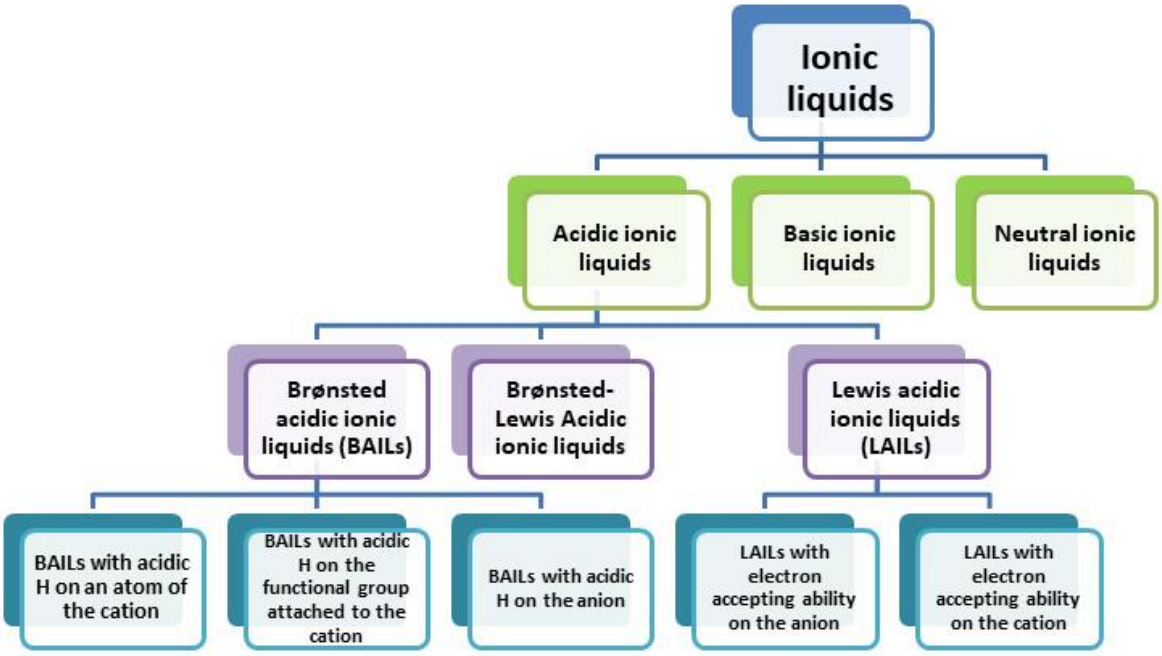

Fig. 1.2: Classification of ionic liquids.

1.1.1 Task-specific ionic liquids

The tethering of an acidic and basic functional group to the cation or anion of an ionic liquid makes them task-specific ionic liquids (TSILs), which are designed for a particular task. For example, attachment of $–SO_3H$ or –COOH groups to the ammonium, pyridinium or imidazolium cations of an organic salt generate the Brønsted acidic TSILs (**Fig. 1.3).** They are known to exist in the liquid state at room temperature irrespective of the position of acidic protons, i.e., either in the cation or in the anion (excluding the anions of complex metal halides). Sarma et al. (2017) reviewed the synthesis and catalytic uses of task-specific $–SO_3H$ functionalized ILs (SFILs) [25]. There are two types of SFILs based on the position of the $–SO_3H$ group in the cationic component: (a) N-alkyl $–SO_3H$ functionalized ILs and (b) direct N-SO_3H functionalized ILs as shown in **Fig. 1.3.** Some of the earlier reports on the direct N-SO_3H functionalized ILs reveal their high thermal stability as well as Brønsted acidity [9, 10, 26]. These properties made them suitable candidates to be used in organic transformations [9, 10, 25, 26].

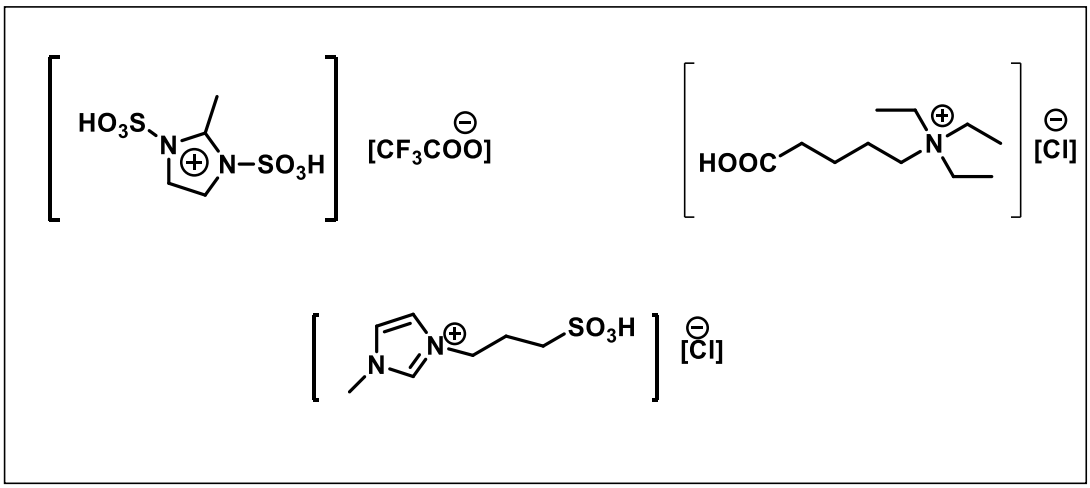

Fig.1.3: Structures of some task-specific ionic liquids (TSILs).

1.1.2 Halometallate ionic liquids

In most cases of Lewis acidic ionic liquids (LAILs), the electron accepting ability lies in their anions which are mainly halometallate ILs [7]. These halometallate ILs are obtained from the reaction between a halide containing IL and a Lewis-acidic metal halide at various molar ratios. The composition of such ILs is typically reported as the molar ratio of metal halide, χMXm, **Equation 1.1** [27]**.**

$$\mathbf{[Cation]X + nMX_m \longrightarrow [Cation][M_nX_{n*m+1}]} \qquad \textbf{(Equation 1.1)}$$

$$\chi\mathbf{MX_m = n/(1+n)}$$

The χMX_m values that yield homogeneous ILs vary depending on the metal and the halide ion. A dynamic equilibrium mixture of various complex metal-halide anions either in molten, semi-solid or in solid states are often generated according to **Equation 1.1**, based on the various molar ratios of the metal halides used. Most of the early reported halometallate ILs were the chloroaluminate ILs, which mainly existed in the liquid state and were highly moisture unstable [27-29]. These ILs contained an equilibrium mixture of chloroaluminate anions such as $AlCl_4^-$, $Al_2Cl_7^-$, and $Al_3Cl_{10}^-$. Shortly after, the halometallate ionic liquids (**Fig.1.4**) of other transition metals like Zn, Sn, Ga, Fe, Co, Ni and lanthanides were also developed [30-35]. They were found to be solid or semi-solid in nature and have less moisture sensitivity. Some of them were also obtained as liquids at ambient temperatures.

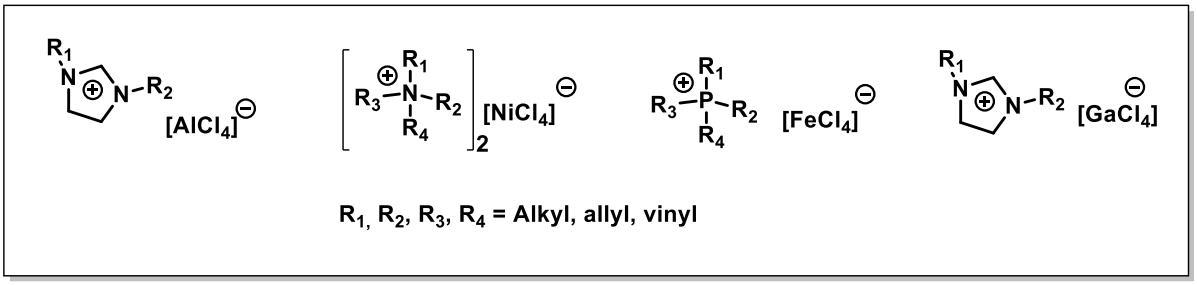

Fig.1.4: Structures of some Lewis acidic halometallate ILs.

Generally, these halometallate ILs are Lewis acidic in nature. However, dual-functionalized halometallate ILs are also known to exist that contain both the Brønsted and Lewis acidic functions [33-35]. The Brønsted acidic function in such ILs resides on the cationic part while the anionic part containing complex metal halides is Lewis acidic. In comparison to the Lewis-acidic halometallate ILs, the existence of Brønsted acidic function in the organic cation enriches them with several advantages such as higher thermal stability and stability to moisture by facilitating strong electrostatic interaction within the ion-pair. The dual-functionalized ILs are also obtained in the solid or semi-solid state at ambient temperatures and have higher melting points than the organic salts. Some of them are readily utilized as heterogeneous catalysts in several organic reactions as well as precursors in nanoparticle synthesis. **Fig. 1.5** shows representative ILs belonging to this class.

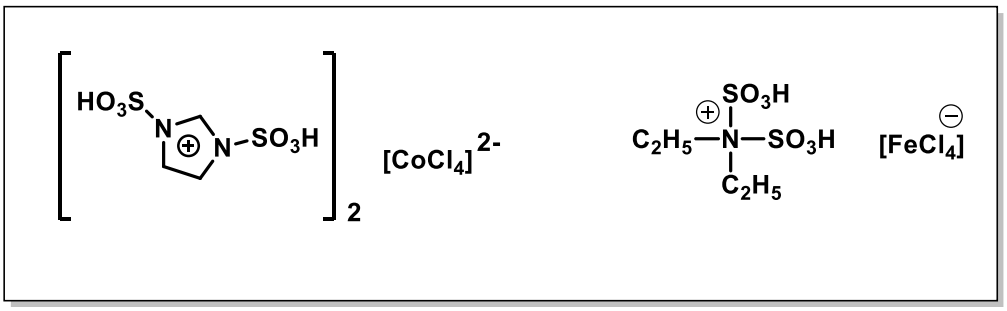

Fig.1.5: Structures of some Brønsted-Lewis acidic halometallate ILs.

1.2 Physicochemical and electrochemical properties of acidic ionic liquids

As a designer solvent, ionic liquids offer the advantage of tuning their physicochemical properties through making suitable combinations of constituent organic cations and inorganic/organic anions, as mentioned in section 1.1 [5].The study of physicochemical and electrochemical properties of the ILs is essential to find their appropriate

applications in specific fields. The information regarding the ionic associations, solvent-ion interactions etc. can be found from their transport properties and is vital for electrochemical applications [36]. Likewise, the knowledge of molecular structures can help in identifying their effects on the physicochemical properties and then proper uses in specific areas [37]. In this section, we briefly cover a discussion of conductivity, thermal stability, density, acidity, viscosity, surface tension, surfactant-like properties, solvatochromic parameters and electrochemical stability of the acidic ILs (AILs) including the TSILs.

1.2.1 Conductivity of ILs

Room temperature acidic ionic liquids (RTAILs) are known to have conductivity values as high as 20 $mScm^{-1}$[38]. These values are often affected by several factors like temperature, concentration, type of ions, ion size and mobility, ionic charge delocalization, aggregation of ions, presence of solvents, viscosity, density, etc. It has been observed that the ionic conductivity of imidazolium based ILs is higher than ammonium based ILs [7, 39]. This is due to the charge delocalization on the aromatic imidazolium ring, which reduces the electrostatic interactions between the constituent ions as compared to the charge-localized ammonium ions or saturated rings with a localized charge on the nitrogen atom [7, 39]. The reduction of electrostatic interactions between the ions, results in lower viscosities of imidazolium ILs than those of quaternary ammonium ILs. The conductivity and viscosity of an IL are inversely proportional, and this relationship can be described using the Walden rule **(Equation 1.2)** [40].

$$\Lambda\eta = \text{Constant} \qquad \textbf{(Equation 1.2)}$$

Where, η is the viscosity and Λ is the molar conductivity of the IL. The plot of log Λ against log η^{-1} is known as the Walden plot and is used as a measure of the tendency of ionic liquids, molten salts or non-aqueous electrolytes to form ions. A reference line established by dilute KCl solutions is considered to be the 'ideal' representing independent ions without any interionic interactions. The proximity of the plotted values to the KCl reference line is an indicator of the interionic interactions between IL anions and cations. Ionic liquids whose Walden plot values are near the reference line show more tendencies to form individual ions, compared to those ILs whose Walden plot values located away from the reference KCl line [29]. The extent of ionicity of an ionic liquid can be measured in terms of ΔW, the vertical distance to the KCl line [29, 40, 41].

The Walden plot values below the ideal line indicate ion aggregation and thus less ionic conductivity values for the ILs. **Fig.1.6** shows a representative Walden plot.

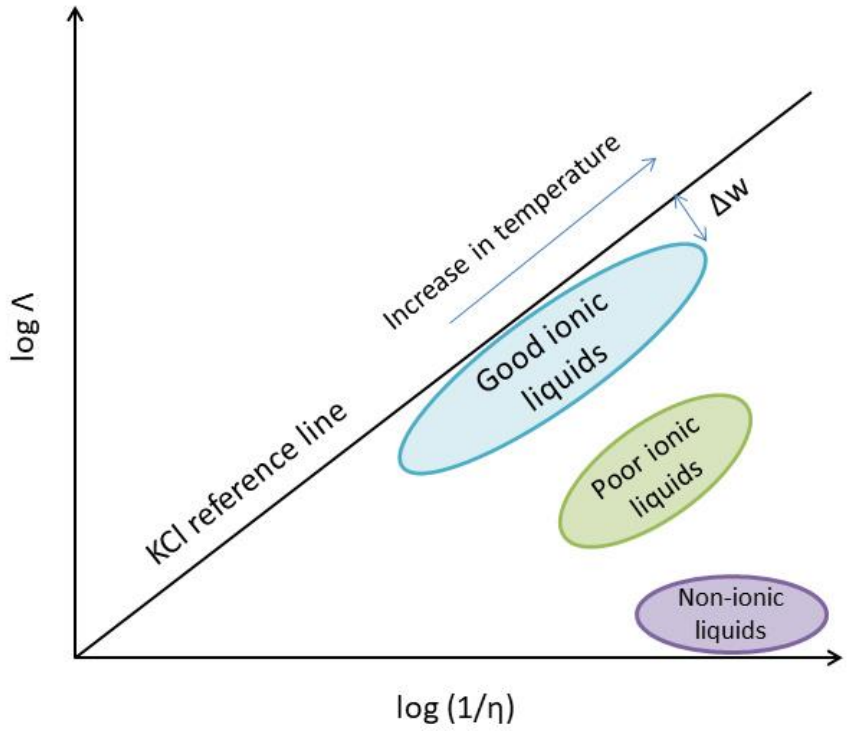

Fig. 1.6: Representative Walden plot indicating the positions of good ILs, poor ILs and non-ionic liquids.

Zhou et al. examined the electrochemical stability and ionic conductivities (σ) of the imidazolium-based mono-ether functional ionic liquids and correlated the results with the cation and anion structures **(Fig.1.7)** [42]. Ionic conductivities of these ILs were dependent on the size of anions and followed the order $[NTf_2]^-$ > $[BF_4]^-$ > $[PF_6]^-$ [42].

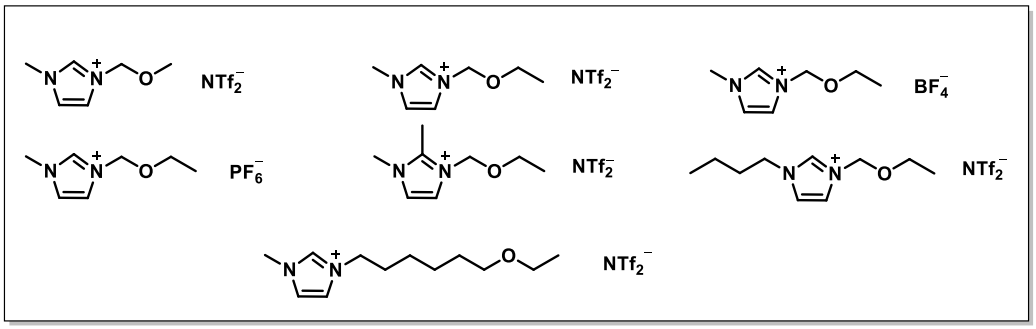

Fig.1.7: Structures of mono-ether functionalized ILs.

A similar effect of the anion size on the ionic conductivities was observed for another series of imidazolium based acidic ILs [HMIM][HCOO], [HMIM][CH_3COO], [HMIM][CH_3CH_2COO], and [HBIM][CH_3COO] in water, DMSO, and ethylene glycol (**Fig. 1.8**) [43]. The conductivity values decrease in the order [HMIM][HCOO]>[HMIM][CH_3COO]>[HMIM][CH_3CH_2COO]>[HBIm][CH_3COO] in all the molecular solvents studied. This can be attributed to the increase in the ionic association of the cations with the anions with increasing size of the anions, which follows the order: $[HCOO]^-$<$[CH_3COO]^-$<$[CH_3CH_2COO]^-$. The +I inductive effect of the ethyl group makes the $[CH_3CH_2COO]^-$ anion highly unstable and thus prompts it to have higher interactions with the cation for minimizing its instability through ionic association. In comparison to $[CH_3CH_2COO]^-$, the $[HCOO]^-$ and $[CH_3COO]^-$ ions are more stable and thus, have less tendencies for ionic association. Also, the increasing size of cations in the order: [HMIM]<[HBIM], decreases their mobility (μ) and hence their conductivities [43].

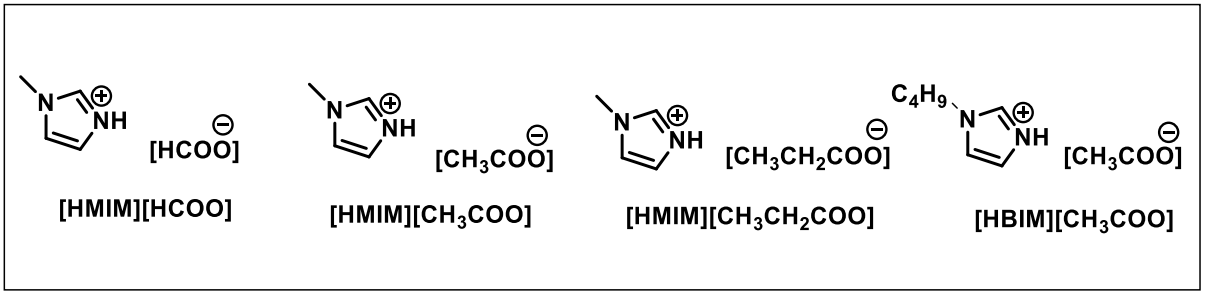

Fig. 1.8: Structure of imidazolium-based carboxylate ILs.

Subsequently, it was found that the addition of molecular solvents to pure RTAILs helps us to obtain binary mixtures of higher conductivities and lower viscosities than pure RTAILs. On addition of solvent, the mobility of the charge carriers increased due to reduced viscosity, and this led to an increase in their conductivities [41,44]. The polarity of the solvent used also influences the conductivity of the ILs. Thawarkar et al. measured the conductivities of three acidic ionic liquids (AILs) ([HMIM][HCOO], [HMIM][CH_3COO] and [HMIM][CH_3CH_2COO] (**Fig. 1.8**) in six molecular solvents namely water, methanol, ethanol, dimethyl sulfoxide, nitrobenzene, and acetonitrile, at 298.15 K and correlated the results with the solvent polarity using the solvatochromic parameters (E^T_N, α, and β) of the solvents [45]. The conductivity values for all these protic ionic liquids (PILs) increases with rising polarity of the molecular solvent [45].

The conductivity of ILs is also affected by temperature and the general trend is that the conductivity increases with increasing temperature. This can be attributed to the fact that with the rise of temperature, the interionic attraction decreases hence the mobility increases [29]. Furthermore, the ionicity increases with the decrease of interionic attraction and hence, the number of free ions available for conduction increases with rising of temperature [29]. Thawarkar et al. later employed conductometry and NMR studies to study the ionicities of the binary mixtures of nine protic and aprotic imidazolium ionic liquids in three molecular solvents namely water, dimethyl sulfoxide, and ethylene glycol within the temperature range of 293.15–323.15 K **(Fig. 1.9)** [43]. Greater ionicities of the aprotic imidazolium ILs compared to those of the protic imidazolium ILs were observed [43]. In these solvents, the conductivity of ILs expressed a typical temperature dependent Arrhenius behaviour.

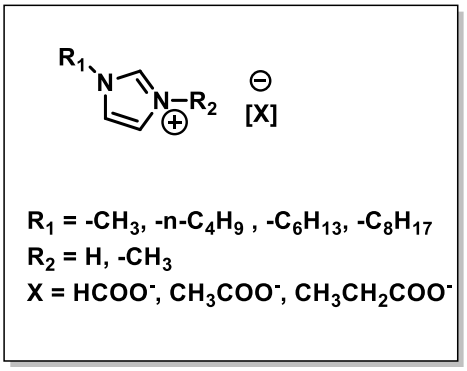

Fig. 1.9: General Structure of imidazolium carboxylate ILs.

A similar result was reported by Anouti et al. for aqueous solutions of RTAILs [Pyrr][$MeSO_3$] and [DIPEA][$MeSO_3$] (**Fig. 1.10**) within the temperature range of 25-80°C. The conductivity values of [Pyrr][$MeSO_3$] and [DIPEA][$MeSO_3$] increased from 29 to 65.8 $mScm^{-1}$ and from 50 to 120 $mScm^{-1}$ with the rise in temperature [44].

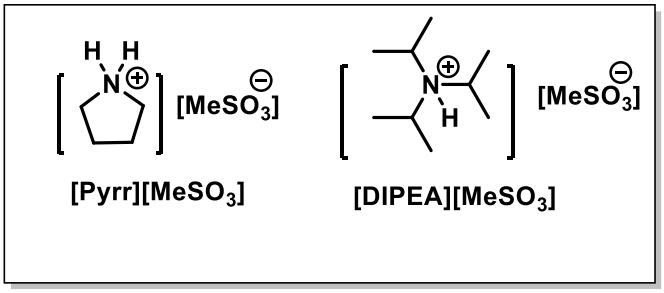

Fig. 1.10: Structures of the ILs [DIPEA][$MeSO_3$]and [Pyrr][$MeSO_3$].

1.2.2 Thermal stability of the ILs

High thermal stability of the ILs enables their applications to be used as electrolytes in fuel cells, batteries and as catalyst in high temperature reactions. The thermal stability of the ILs mainly depends on the nature of the constituent ions. For instance, imidazolium cation based ILs are found to be thermally more stable than those with tetralkylammonium cations [29, 46]. Amarasekara et al. reported the thermal properties of a total of 24 imidazolium-, triethanolammonium- and pyridinium-type $–SO_3H$ group functionalized room-temperature BAILs (**Fig. 1.11**) using thermogravimetric analysis [46]. The thermal stability of the ILs decreases in the order: methylimidazolium > triethanolammonium > pyridinium. Subsequently, for the series of $–SO_3H$ functionalized methylimidazolium BAILs, the thermal stability significantly depended on the nature of the anion and decreased in the order: $CH_3CO_2^->SO_4^{2-}>PO_4^{3-}>BF_4^->CH_3SO_3^->Cl^->Br^-$. For the pyridinium and triethanolammonium BAILs a similar thermal stability order for the anions was observed: $CH_3CO_2^- = SO_4^{2-}>PO_4^{3-}>BF_4^->CH_3SO_3^->Cl^->Br^-$ [46].

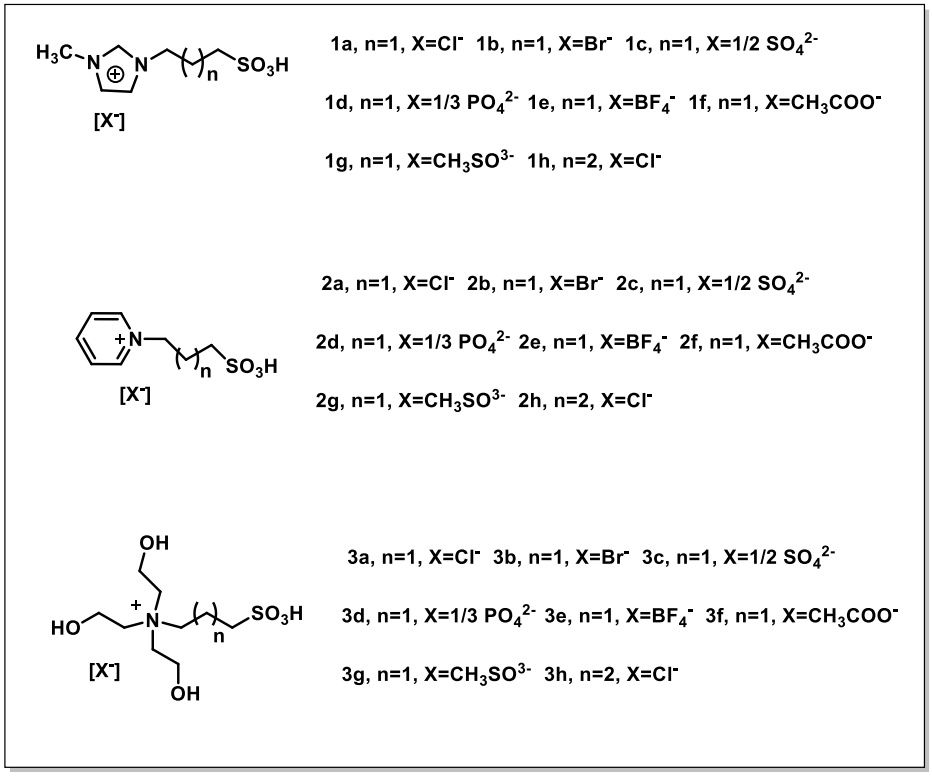

Fig.1.11: Structures of the $–SO_3H$ group functionalized room-temperature BAILs.

The halometallate ILs are known to be more thermally stable compared to the BAILs, due to the presence of inorganic metal-halide ions in their structure. Kalita et al.

investigated the thermal stability of a series of N, N′-disulfopiperazinium chlorometallates of Fe(III), Ni(II) and Co(II) (**Fig. 1.12**) [33]. Thermogravimetric analyses of the chlorometallates revealed the removal of physisorbed water from the chlorometallates around 100 °C for Fe(III) salt in contrast to 150-170 °C for Ni(II) and Co(II) organic salts for strongly bound water molecules in highly crystalline state. The Fe(III) salt showed thermal stability up to 220 ℃, whereas the Ni(II) and Co(II) salts were found to be thermally stable up to 280-300 ℃ [33].

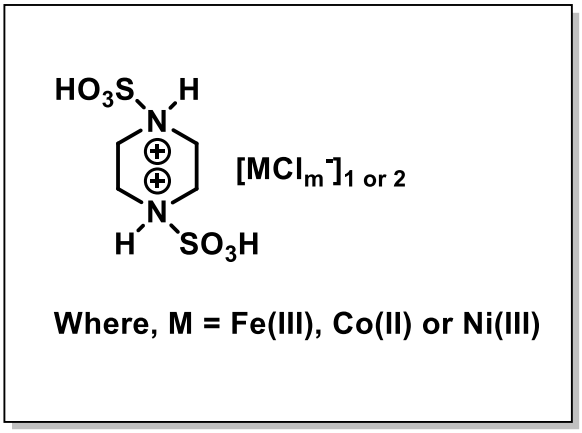

Fig. 1.12: Structures of N, N′-Disulfopiperazinium Chlorometallates.

Another study by Hajipour et al. supported the above observation about higher thermal stabilities of Lewis acidic ionic liquids (LAILs) [47]. The thermal stabilities of a series of Lewis acidic ionic liquids ([Bu_3NBn]Cl-2($AlCl_3$), [Bu_3NBn]Cl-2($CuCl_2$), [Bu_3NBn]Cl-2($FeCl_3$) and [Bu_3NBn]Cl-2($SnCl_4$), [Bu_3NBn] Cl-2($ZnCl_2$), **(Fig. 1.13)** were analysed using TGA technique [47]. [Bu_3NBn] Cl-2($FeCl_3$) was found to be the most thermally stable among the five LAILs. Its first weight loss of about 5% took place at 329.69 °C, which was followed by another weight loss of about 10% at 339.9 °C. Whereas, [Bu_3NBn]Cl-2($AlCl_3$) was revealed to be the least thermally stable and showed its first decomposition at 128.24 °C. The decreasing order of thermal stability of the five ILs is: [Bu_3NBn] Cl-2($FeCl_3$)> [Bu_3NBn]Cl-2($CuCl_2$)> [Bu_3NBn]Cl-2($SnCl_4$)> [Bu_3NBn] Cl-2($ZnCl_2$)> [Bu_3NBn]Cl-2($AlCl_3$) [47].

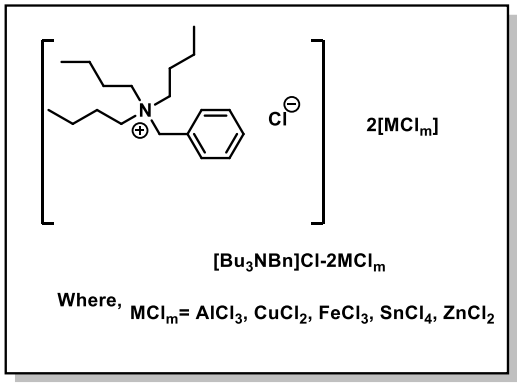

Fig. 1.13: Structures of the [Bu_3NBn]Cl-2(MCl_m) LAILs.

1.2.3 Electrochemical stability of the ILs

The presence of large number of charge carriers in the ionic liquids makes them suitable candidates for their application as electrolytes in energy conversion devices like batteries, fuel cells etc. Hence, the knowledge regarding the electrochemical stability of ILs is of utmost importance for their future applications. The electrochemical stability of the ionic liquids is measured in terms of electrochemical stability window (ESW) or electrochemical window (EW), which is defined as the potential range within which the substance is electrochemically inert, i.e. it is neither oxidized nor reduced [48]. It is calculated according to **Equation 1.3** [48].

$$\mathbf{ESW = E_{ANODIC} - E_{CATHODIC}} \qquad \textbf{(Equation 1.3)}$$

The ESW of the ILs are usually measured using techniques like linear sweep voltammetry (LSV) and cyclic voltammetry (CV). The EWs of some typical ILs are found in the range of 4.5–5 V [7]. There are several factors affecting the ESW of the ILs which include nature of the constituent ions, presence of impurities or additives, solvents, nature of the working electrodes, scan rates, etc. It is generally observed that the quaternary ammonium ILs have higher ESW compared to the imidazolium ILs [29]. However, the presence of alkyl side chains is also known to increase the redox stability in imidazolium ILs.

Wu et al. studied the effect of constituent ions on the ESW of the ILs using cyclic voltammetry technique [36]. Nine cyclic amine-based BAILs containing pyrrolidinium, piperidinium or azepanium units as cations, and formate, trifluoroacetate, or hydrogen

sulfate groups as anions, were synthesized and their ESWs were evaluated (**Fig.1.14)**. These ILs exhibited large ESWs (3.22–3.99 V) [36]. The cathodic stability of these ILs depends upon the reduction potential of the cation. The reduction of cation is expected to proceed by the concerted-exchange (CE) mechanism involving deprotonation of the positively charged nitrogen in the pyrrolidinium, piperidiniuim, or azepanium ring followed by the reduction of the proton to H_2. The reduction or cathodic potential of these cations were not influenced by the cation size or with the presence of N-methyl substituents. All of them exhibited identical cathodic potentials at around -2.5 V. The anodic stability of the ILs was determined by the oxidation potential of the anions. It was observed that, compared to the hydrogen sulfate anion (+1.5 V), the formate and trifluoroacetate anions were oxidized at a relatively lower anodic potential of +0.7 V. The higher anodic potential of the hydrogen sulfate can be attributed to formation of persulfate ion on the oxidation of the hydrogen sulfate anions. Thus, hydrogen-sulfate-based ILs have larger EWs (3.98–3.99 V) than those of the formate- and trifluoroacetate-based ILs [36].

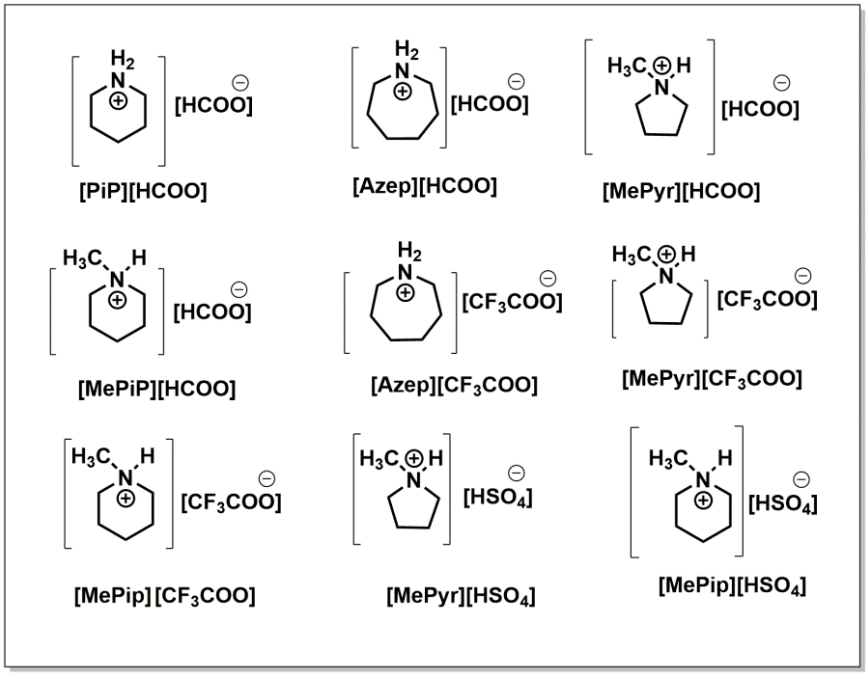

Fig. 1.14: Structures of cyclic amine based Brønsted acidic ILs.

The presence of water as an impurity is also known to affect the ESW of the ILs. Stettner et al. evaluated the ESWs of pure 1-butylpyrrolidinium bis(trifluoromethanesulfonyl)imide (Pyr_{H4} TFSI) (**Fig. 1.15**) and its binary mixtures with different percentages of water (2% and 3.8%) at 40 °C using both the LSV and CV

techniques [49]. It was found that the anodic limit was strongly affected by the water content and the anodic potentials (vs. Ag) decreased with the increase of water content, i.e. 1.5 V for the mixture containing 3.8% water, 1.75 V with 2% water and 2 V with 1% water content [49].

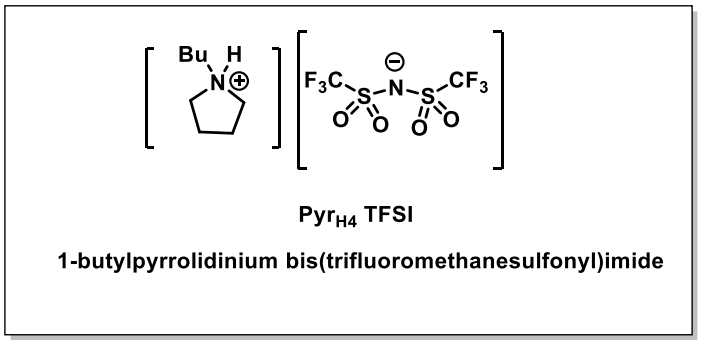

Fig. 1.15: Structure of Pyr_{H4} TFSI.

Shmukler et al. studied the effect of temperature on the ESW of the acidic ionic liquids (AILs). The ESWs of triethylamine based AILs ([TEA][PTSA], [TEA][TFA] and [TEA][H_2PHO_3]) (**Fig. 1.16**) were measured at different temperatures (50, 70, 90 and 120°C) [50]. The largest ESWs were obtained at 50 °C for all the three AILs. It was observed that the reduction of the triethylammonium cation was dependent on the nature of the counter anion. The cathodic limit potentials of [TEA][TFA], [TEA][PTSA] and [TEA][H_2PHO_3] ILs at 50 °C were found to be -0.75, -0.85, and -0.45 V, respectively [50]. The EWs of the three ILs became narrower with the rise in temperature which can be related to the influence of temperature on kinetics of the redox processes involved. Out of the three ILs, [TEA][H_2PHO_3] was the most sensitive to the increase of temperature from 50 to 120 °C and the potential range of its electrochemical stability decreased by about 700 mV within this temperature range [50].

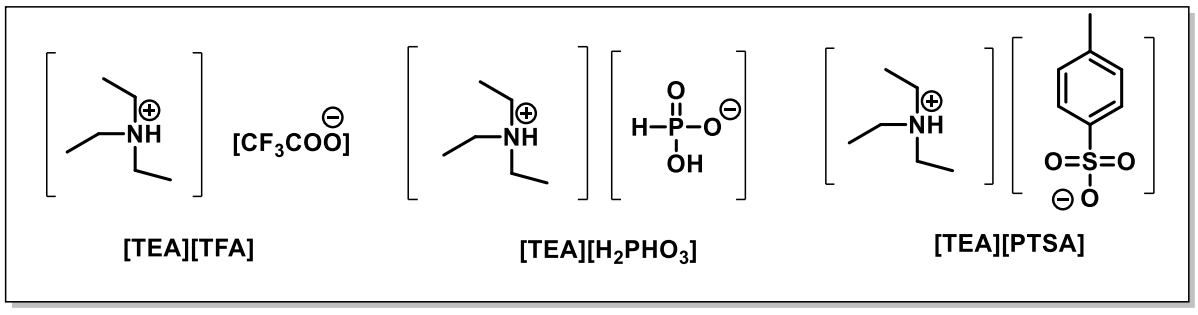

Fig. 1.16: Structures of triethylamine based AILs.

1.2.4 Acidity of the ILs

Acidity of the ILs is a necessary criterion to determine their applications as catalysts in several organic transformations. Like the previously discussed properties, the acidity of the ILs is also a function of their constituent ions. The Brønsted acidity of the ILs is usually determined by evaluating their Hammett functions (H^o) using UV-Vis spectroscopy [9, 26, 51].

The Hammett function values (H^o) for BAILs can be calculated from the UV–Vis absorbance of a basic indicator (I), such as 4-nitroaniline in water (or alcohol), before and after the addition of a BAIL, by using **Equation 1.4**:

$$\mathbf{H^o = pK(IH^+)\ (aq) + log[I]/[IH^+]} \qquad \textbf{(Equation 1.4)}$$

where $pK(IH^+)$ (aq) is the pKa value of the basic indicator in aqueous solution and the $[I]/[IH^+]$ is the ratio of absorbance of the indicator measured before and after addition of the

ILs. The typical procedure involves mixing equal concentrations of 4-nitroaniline indicator (5mg dm^{-3}, pKa = 0.99) and BAIL (5 mmol dm^{-3}) in ethanol or water solution. The absorbance of the basic indicator [I] in the solutions decreases with the increasing acidity of the BAIL. This is because of the lower molar absorptivity of the protonated form of the indicator [HI^+], which never appeared in the spectra [26]. Thus, with the increasing acidity of the BAILs, their H^o values become smaller.

Thomazeau et al. evaluated the Brønsted acidity of three ionic liquids [BMIM][NTf_2], [BMIM][BF_4], and [BMMIM][BF_4] **(Fig. 1.17)** by determining their Hammett acidity functions (H^o) using UV-visible spectroscopy [51]. The acidity of the ILs decreased in the following order [BMIM][NTf_2]>[BMIM][BF_4]>[BMMIM][BF_4]. The increasing +I effect of C-2 methyl substituent of the imidazolium cation in [BMMIM][BF_4] decreased its electron deficient character and hence its acidity is lower compared to the two [BMIM] ILs [51].

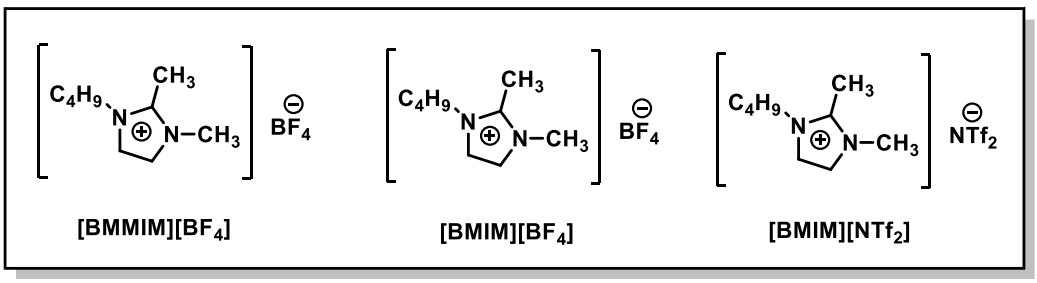

Fig. 1.17: Structure of the [BMIM] and [BMMIM] ILs.

A Hammett acidity study was conducted by Dutta et al. for a series of 1,3-disulfonic acid imidazolium carboxylate ionic liquids [DSIM][X] where X=[CH_3COO^-], [CCl_3COO^-] and [CF_3COO^-] (**Fig. 1.17**) [26]. The acidity order of the BAILs was found to increase in the order: [DSIM][CH_3COO] < [DSIM][CCl_3COO] < [DSIM][CF_3COO]. It is found that acidity of the BAILs increases with decreasing pKa values of the corresponding carboxylic acids: CH_3COOH (2.2), CCl_3COOH (1.6), CF_3COOH (1.2) [26].

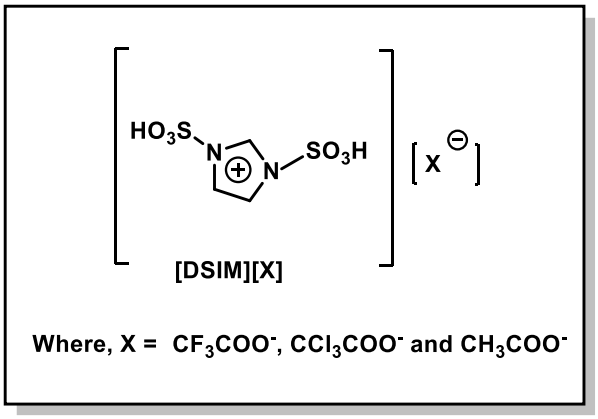

Fig. 1.18: Structure of 1,3-disulfonic acid imidazolium carboxylate ionic liquids [DSIM][X].

The Lewis acidity of the ILs is measured by the Gutmann Acceptor Number (AN) approach using ^{31}P NMR, [27] and FT-IR band shift of a pyridine probe molecule [52, 53]. The Gutmann Acceptor Number (AN) approach measures the AN using ^{31}P NMR chemical shift of a triethylphosphine oxide (TEPO) probe molecule dissolved in the respective IL using **Equation 1.5**.

$$\mathbf{AN = 2{:}348\ \delta_{inf}} \qquad \textbf{(Equation 1.5)}$$

^{31}P NMR spectra of TEPO at several small concentrations are recorded, and these data are then extrapolated to infinite dilution, from which a value of δ_{inf} (^{31}P chemical shift at infinite dilution of TEPO) is deduced. Coordination of the TEPO with a Lewis-acidic site induces a change in its ^{31}P NMR chemical shift which is directly proportional to AN [53]. An arbitrary scale is defined based on the ^{31}P NMR chemical shift of the probe molecule in hexane (AN=0) (less acidic) and antimony (V) chloride ($SbCl_5$) in 1,2-dichloroethane (AN=100) (highly acidic). Estager et al. used this approach to determine the Lewis acidity of a range of

chlorometallate(III) ILs, based on Group 13 metals (Al(III), Ga(III) and In(III)) and 1-octyl-3-methylimidazolium chloride ([C_8MIM][Cl]), at differentcompositions (χMCl_3 =0.25–0.75) (**Fig.1.19**) [53]. The AN value for the chloroaluminate systems ($\chi AlCl_3$ =0.33–0.67) lay in the range of 93.19–95.95; for the chlorogallate ($\chi GaCl_3$ =0.33–0.5) the AN values were in the range of 21.65–45.85. However, the chlorogallate(III) IL with ($\chi GaCl_3$ = 0.75) exhibits a very high AN of 107.47. The chloroindate(III) ILs exhibit rather low AN values of (32.53–58.36). This variation in the acidity of the three classes of the chlorometallate ILs is attributed to the formation of different metal-chloride complex (MCl_3, MCl_4^-, $M_2Cl_7^-$,MCl_5^-,MCl_6^-, etc.) at different compositions(χMCl_3) for each class[53].

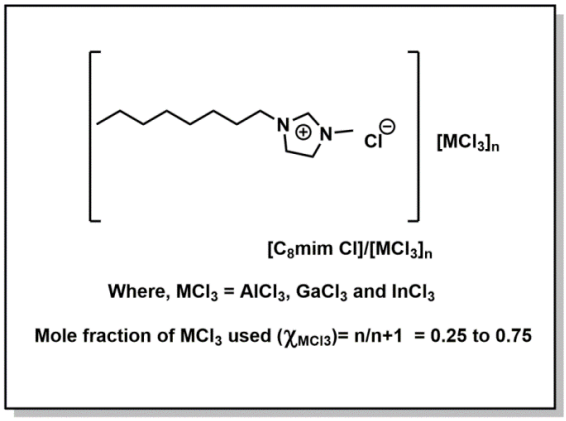

Fig.1.19: Structure of the [C_8mim][Cl]-chlorometallates.

Duan et al. utilised the FT-IR spectroscopy technique with pyridine as the probe molecule to determine the Lewis acidity of a series of ILs prepared from $ZnCl_2$ with choline chloride, and $ZnCl_2$ with benzyltrimethylammonium chloride, in different molar compositions (**Fig. 1.20**) [54]. The samples for IR analyses were prepared by mixing the pyridine probe and the Lewis-acidic IL in the mass ratio of pyridine: LAIL = 1:3, and the FT-IR spectra of these samples were then recorded. The Lewis acidity was determined by monitoring characteristic IR bands of the pyridine molecule within the 1400–1700 cm^{-1} region. The FT-IR spectra of neat pyridine shows a band near 1437 cm^{-1}. The presence of a band near 1450 cm^{-1} indicates the coordination of pyridine to the Lewis-acidic site and this band shifts to higher values with increase in the Lewis acidity of the IL. The pyridine band shifted from 1437 to 1448cm^{-1} for the choline chloride:x $ZnCl_2$ (x=1, 2, 3) and benzyltrimethylammonium chloride:2$ZnCl_2$ ILs,
indicating the coordination of pyridine to the Lewis-acidic site and the similar Lewis-acidic strength of the LAILs [54].

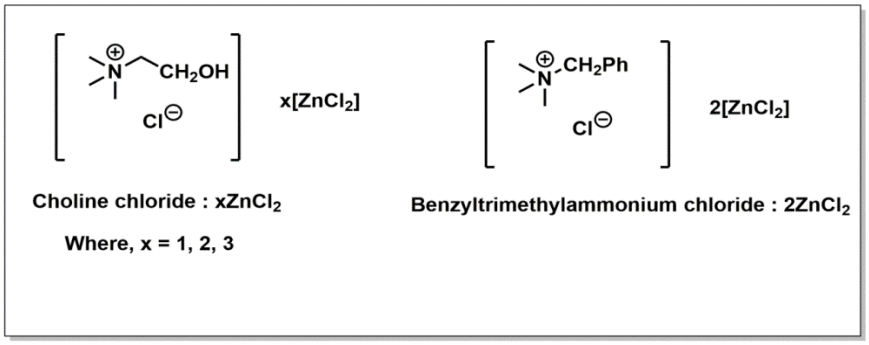

Fig.1.20: Structure of chlorozincate LAILs.

1.2.5 Viscosity of the ILs

Viscosity of the ILs is another important property determining their electrochemical applications. The viscosity of the ILs also influences other transport properties like their conductivity and the mobility of the ions. The factors affecting the viscosity of the ILs include the strength of their van der Waals interactions, hydrogen bonding ability, and planarity of molecular structures [7, 29, 55]. The imidazolium ILs are less viscous than the quaternary ammonium ILs because of their planar structure. The planarity allows relatively facile slip between the molecules, thus making them less viscous. Furthermore, the charge delocalization on the imidazolium ring reduces the electrostatic interactions with the constituent ions than the ammonium ions or saturated rings with a localized charge on the nitrogen atom, thus making the imidazolium ILs less viscous [55]. However, the presence of alkyl side chains increases the viscosity of both the imidazolium as well as ammonium ILs [55, 56].

Keshapolla et al. measured the dynamic viscosities of a series of protic trihexylammonium (THA) and trioctylammonium (TOA) ILs (**Fig. 1.21**) at different temperatures [57]. It was found that the viscosity of the studied PILs increased with increase in the chain length of cation or anion in the following order: [THA][But]<[THA][Hex]<[THA] [Oct]<[TOA][But]<[TOA][Hex]<[TOA][Oct] [57]. This increase in viscosity can be attributed to the increase of the van der Waals interactions with the increase in the alkyl chain length both in the cation and anion.

Wu et al. studied the effect of temperature on the viscosity of a series of cyclic amine based Brønsted acidic ILs (**Fig. 1.14**) [36]. The viscosity of the BAILs decreased with increasing temperature and the results were modelled using the VTF equation **(Equation 1.6)** since the relationship between viscosity and temperature was not completely linear.

$$\eta = \eta_o \exp [B/(T-T_o)] \qquad \textbf{(Equation 1.6)}$$

Here, T is the absolute temperature, η_o is an adjustable parameter, B a factor related to the activation energy and T_o is the ideal glass transition temperature [36].

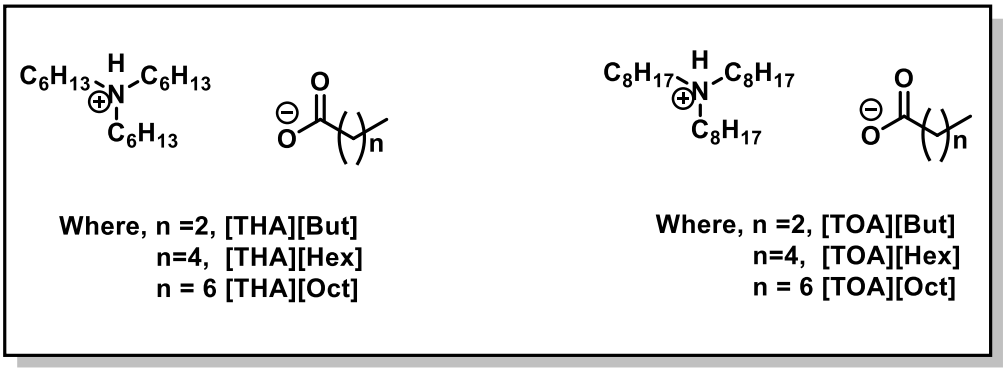

Fig.1.21: Structures of protic trihexylammonium (THA) and trioctylammonium (TOA) ILs.

1.2.6 Density of the ILs

The density of ILs (ρ) is affected by several factors including temperature and ion packing, which again depend on their sizes and shapes as well as the cation-anion interactions. The density of the ILs usually decreases with increasing temperature. Furthermore, at room temperature, increasing chain length of alkyl group of alkylammonium, alkyl imidazolium cations or carboxylate anions decrease the density of ILs [29]. ILs with aromatic cations have higher density values than those with an aliphatic cation because of their higher packing efficiency. The presence of hydroxyl group as a substituent in the cation or the anion of the IL is known to increase the density by an increase in ion-ion interactions because of hydrogen bonding [58].

The effect of increasing the alkyl chain length of carboxylate anions on the density of the ILs was studied by Hanabusa et al. for a series of 1,8-diazabicyclo[5.4.0]-undec-7-ene [DBU]-based RTAILs [59]. Seven RTAILs were synthesized by using DBU as the cation and seven different carboxylic acids HCOOH, CH_3COOH, CH_3CH_2COOH, $CH_3(CH_2)_2COOH$, $CH_3(CH_2)_4COOH$, $CH_3(CH_2)_6COOH$ and $CH_3(CH_2)_8COOH$. Among these seven RTAILs only four ([DBUH][OBu], [DBUH][OHe], [DBUH][OOc] and [DBUH][ODe]) were liquids at room temperature (**Fig. 1.22**). As expected, their densities decreased with the increasing alkyl chain length of the carboxylate anions:

[DBUH][OBu]>[DBUH][OHe]>[DBUH] [OOc]>[DBUH][ODe]. Also, their densities decreased linearly with increasing temperature from 10 to 100°C [59].

The densities of halometallate ILs are however dependent on both the size of the alkyl chain on their cations and also on the mole fraction of the metal-halide ions present (x_{MX}) [29]. It is found that the density of the halometallates usually decreases with the decreasing mole fraction of the metal halide [60]. Zheng et al. studied this effect for two series of Lewis acidic imidazolium chloroaluminates, 1-butyl-3-methylimidazolium chloroaluminate ([BMIM]Cl/$AlCl_3$) and 1-hydrogen-3-methylimidazolium chloroaluminate ([HMIM]Cl/$AlCl_3$) (**Fig. 1.23**), and it was found that their densities decreased with increasing temperature.

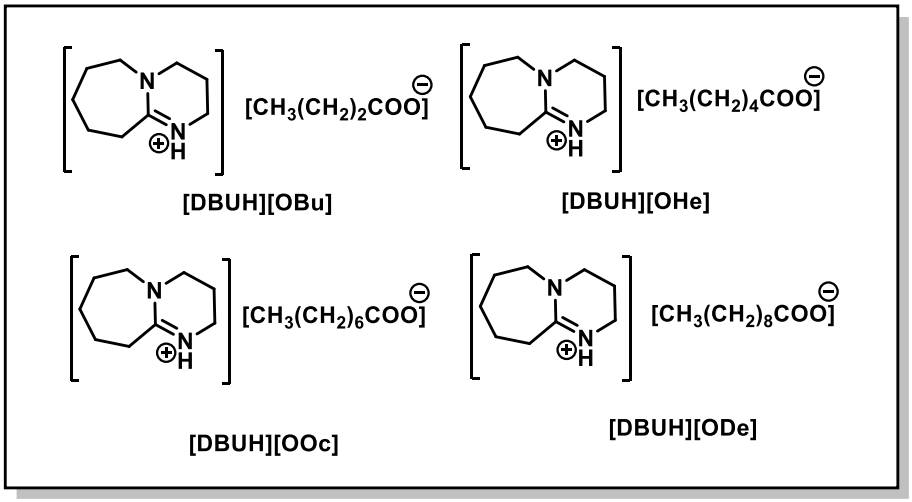

Fig. 1.22: Structure of the DBU ILs.

Additionally, at a given temperature, the density of each LAIL increased with increasing apparent mole fraction of $AlCl_3$ [60]. This can be attributed to the fact that the predominant form of the anion present in [BMIM]Cl.$AlCl_3$/[HMIM]Cl.$AlCl_3$ is $[AlCl_4]^-$, whereas in [BMIM]Cl.$AlCl_3$/[HMIM]Cl.2$AlCl_3$ it is $[Al_2Cl_7]^-$. The concentration of $[Al_2Cl_7]^-$, increases as the apparent mole fraction of $AlCl_3$ increases from 0.50 to 0.67. Thus, the density order is mainly related to the increasing molar concentration of heavier formula-weight anion $[Al_2Cl_7]^-$ in LAILs. Further, it was noticed that the densities of [HMIM] cation containing LAILs were much higher than those of the [BMIM] cation containing LAILs under the same conditions. Hence, it can be concluded that the size of the cations also affects the density of LAILs [60].

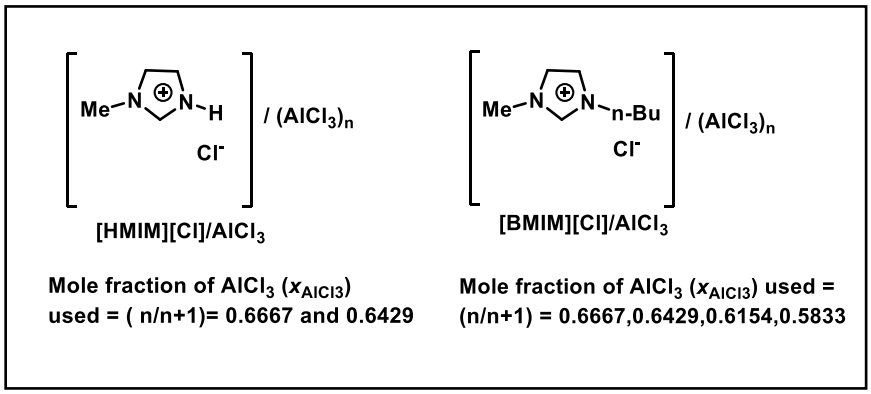

Fig. 1.23: Structures of [BMIM]Cl.$AlCl_3$ and [HMIM]Cl.$AlCl_3$.

1.2.7 Surface tension of the ILs

Investigation of the surface tension of the ILs provides vital information about the fluid properties of the ILs, which are complex and non-isotropic fluids. The surface tension (ɤ) of the ILs is affected by the nature of the constituent ions as well as temperature [29]. The surface tension is usually determined using any of the three methods: Du Noüy ring (DNR) method, pendant drop (PD) method and capillary rise (CR) method.

Ullah et al. investigated the surface tension of seven [HSO_4^-] anion based RTAILs (**Fig. 1.24**), within the temperature range of 293.15–353.15K, using the pendant Drop (PD) method [61]. The surface tension values of the RTAILs at 293.15K were found to be higher than for most common organic solvents but lower than that of water. Furthermore, the surface tension values of the RTAILs decreased with the increasing temperature. Among the seven RTAILs investigated, [HMIM][HSO_4] had the highest surface tension value within the temperature range studied and [MePyr][HSO_4] had the lowest. The high surface tension values of these RTAILs can be attributed to the presence of extensive H-bonding between the cations and the anions which increases the interaction between the ions [61].

Bhattacharjee et al. used the pendant drop method to investigate the effect of temperature and constituent ions on of surface tension of two protic ammonium ILs 2-(dimethylamino)-N,N-dimethylethan-1-ammonium acetate [$N_{11\{2(N11)\}H}$][CH_3CO_2], and N-ethyl-N,N-dimethylammonium phenylacetate, [N_{112H}][$C_7H_7CO_2$] **(Fig. 1.25)** [62]. The surface tension of the [N_{112H}][$C_7H_7CO_2$] was estimated in the temperature range of 293-343K whereas, that of [$N_{11\{2(N11)\}H}$][CH_3CO_2] was estimated in the range 293-323K. The surface tension value obtained at 293.3K was higher in case of [N_{112H}][$C_7H_7CO_2$] (43.6mNm^{-1}) compared to [$N_{11\{2(N11)\}H}$][CH_3CO_2] (33.6mNm^{-1}).

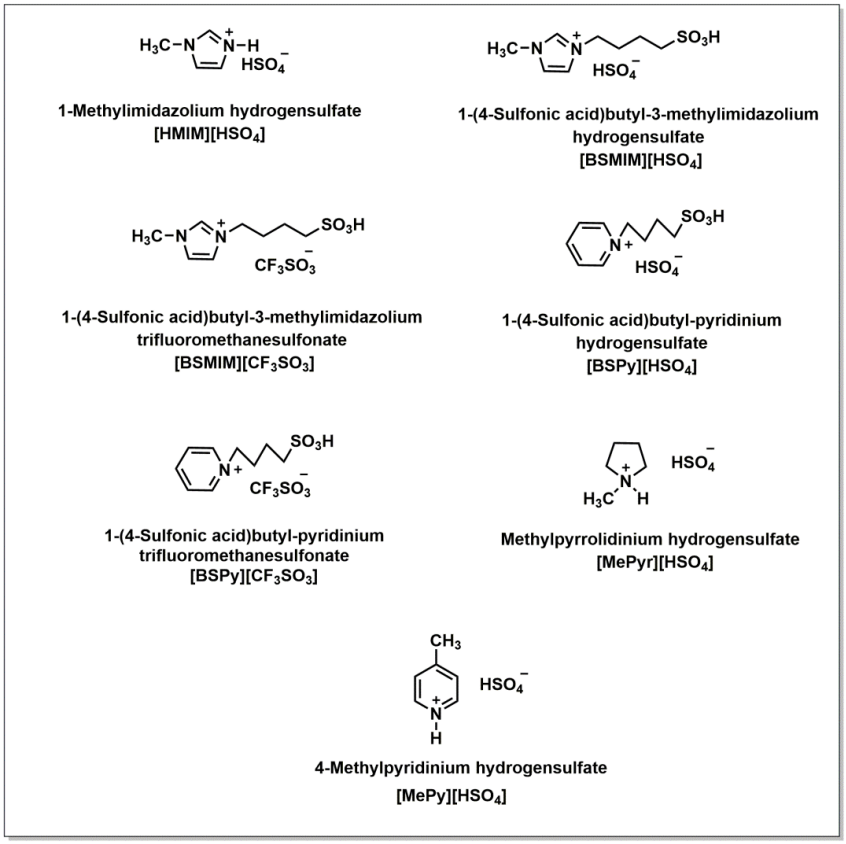

Fig. 1.24: Structures of the seven [HSO_4^-] based RTAILs.

However, surface tension values of both the ILs decreased with increasing temperature. This can be credited to the stronger intermolecular interactions between phenylacetate anion and the smaller [N_{112H}]$^+$ cation, which lead to a more organized arrangement and higher surface tension values compared to [$N_{11\{2(N11)\}H}$][CH_3CO_2] [62].

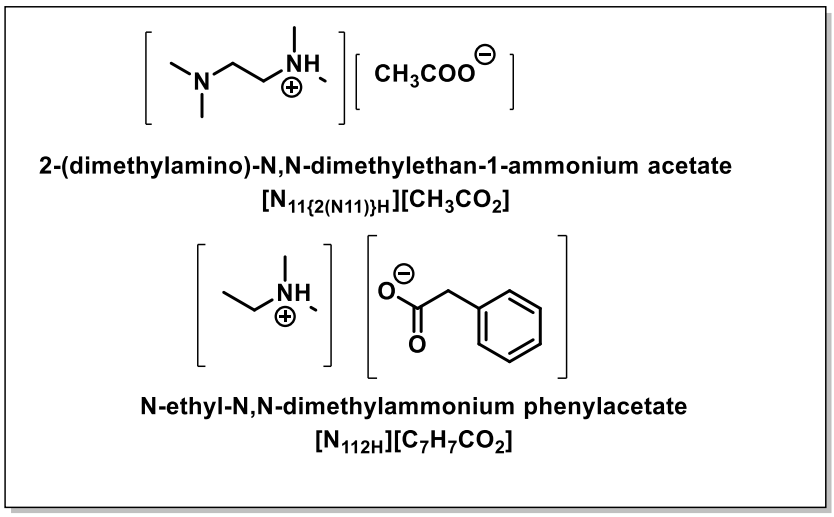

Fig. 1.25: Structures of protic ammonium ILs.

The temperature dependence of surface tension of four $–SO_3H$ functionalized benzimidazolium-based RTAILs **(Fig. 1.26)** were investigated in the temperature range of 293.15–353.15K by Ullah et al. using the pendant drop method [63]. The surface tension values of the four ILs decreased with the increasing temperature. It was found that at a particular temperature, among the four ILs [BSMBIM][CF_3SO_3] had the highest and [BSMBIM][HSO_4] had the lowest surface tension values. Furthermore, at room temperature the surface tension values of all the four ILs were lower than for water but were higher compared to many common organic solvents like methanol, alkanes, etc. [63].

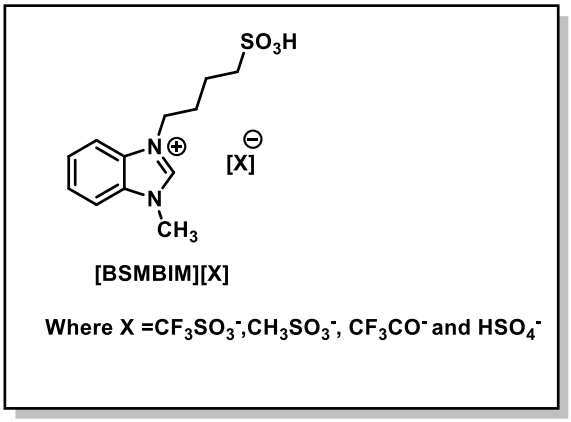

Fig. 1.26: Structure of the [BSBIM] based ILs.

1.2.8 Surfactant-like properties of the ILs

Most of the RTILs are amphiphilic compounds containing distinct hydrophilic and lipophilic molecular fragments, which determine their surface activity and the ability to self-organize in the individual state and in solutions [64-66]. These surfactant-like properties of neat ILs are controlled by the amount of aggregation and complexation between the ions. The aggregation tendencies of the ILs reduce their ionicity.

Several theoretical as well as experimental studies have confirmed the formation of two types of domain by the RTILs: the first one consisting of positively charged cations and negatively charged anions arranging in three-dimensional polar networks supported by strong electrostatic interactions, and the second one comprising of hydrophobic alkyl groups aggregating to form non-polar domains where short-range van der Waals interactions are predominant (**Fig. 1.27**) [66, 67]. RTILs are thus known to display characteristics like that of the classical surfactants.

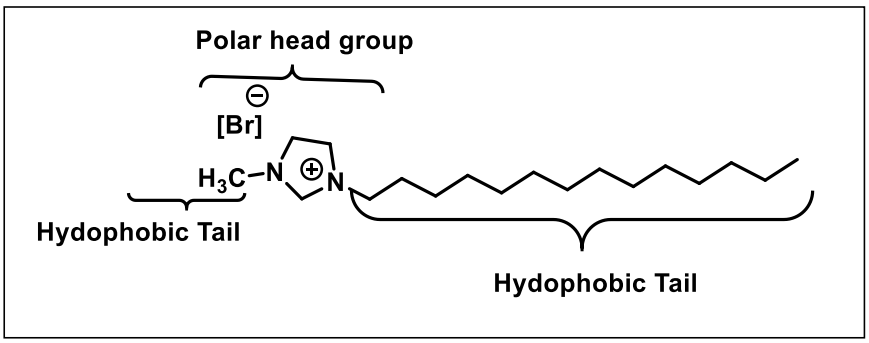

Fig. 1.27: Polar head group and hydrophobic tail of 1-tetradecyl-3-methylimidazolium bromide.

Intensive studies on the process of micellization of ILs in solutions, where the ILs act as surface-active solutes have been conducted, mostly for alkylimidazolium ILs [68]. The sizes of these IL aggregates in solutions are affected by a number of factors like bulkiness of the alkyl substituent and its branching, polar or non-polar nature of the molecular solvents, solution temperature, etc. Polar solvents are known to favour smaller-size aggregates compared to non-polar solvents [69].

Wang et al. studied the aggregation tendencies of some amino acid based protic ionic liquids (PILs) from their Walden plot values [70] **(Fig. 1.28)**. The Walden plot values of most of these PILs lied in the region of poor ionic liquids, indicating aggregation in the ILs.

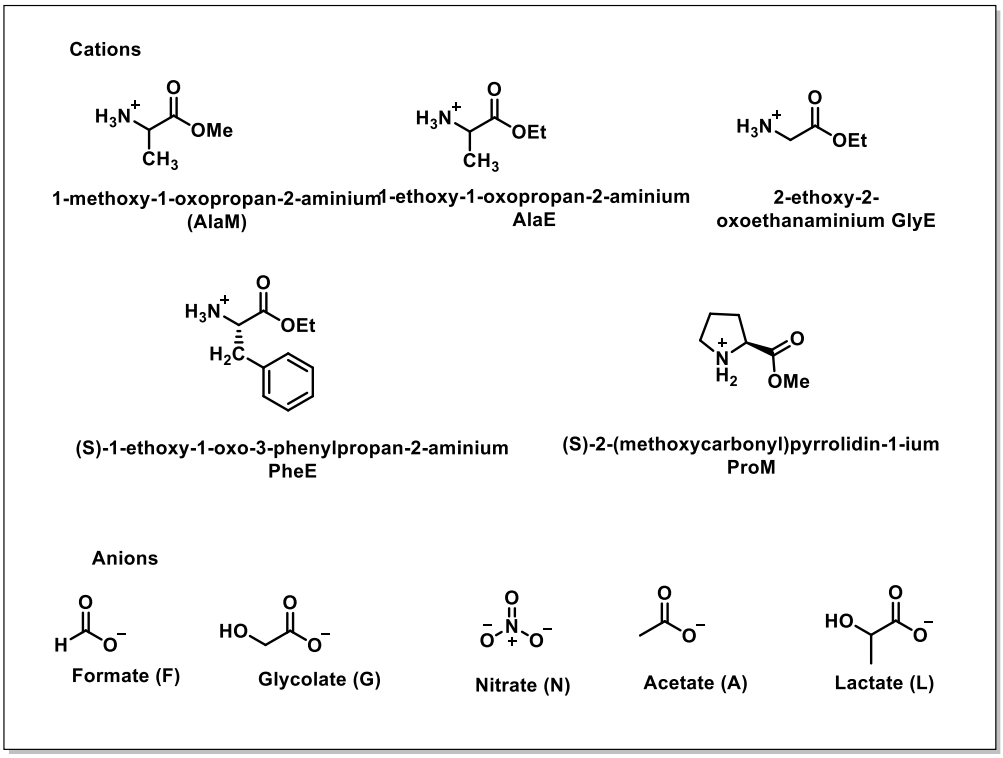

Fig.1.28: Structures of the cations and anions of the PILs.

The PILs, AlaEF and PRoMN were the most ionic, whereas ProMF was found to be the least ionic. Further, the aggregation numbers of these PILs were determined by comparing their molecular weight M_{visc} based on the viscosity with their actual molecular weight M_W. The aggregation numbers obtained for these PILs range from 3.16 to 4.37 [70].

Srinivasa Rao et al. investigated the aggregation properties of room temperature amino acid-based ionic liquids (AAILSs) (**Fig. 1.29**) and correlated the results to the structure of the amino acids [71]. The self-aggregation tendency of these AAILs in aqueous solution was evaluated through measurements of surface tension, conductivity, steady-state fluorescence, dynamic light scattering (DLS), and transmission electron microscopy (TEM). The tensiometry technique was used to analyse the variation of surface tension (γ) as a function of concentration for the various AAILSs at 298. 15K. It was found that, γ decreased with the increasing concentration of AAILSs before reaching a minimum at the critical association concentration (CAC), and after that a nearly constant value of γ was obtained. The CAC values of the AAILSs obtained from surface tension measurements increased in the order $GluC_3LS<ValC_3LS<ProC_3LS<AlaC_3LS<GlyC_3LS$ [71]. This can be correlated to the hydrophobicity and size of the amino acid cations. The higher hydrophobicity and large hydrodynamic size of the $GluC_3$ cation allowed $GluC_3LS$ to form aggregates at lower concentration, whereas $GlyC_3LS$ formed aggregates at comparatively higher concentration due to the less hydrophobic nature and smaller size of the $GlyC_3$ cation. Further, conductometric studies were performed on the aqueous solutions of these AAILs and CAC values obtained from the conductometric studies agreed with those obtained through tensiometry [71].

Later on, Yang et al. also studied the aggregation of behaviour of three amino acid anion based ionic liquids (AAILs) $[C_{14}mim][Ala]$, $[C_{14}mim][Pro]$,and $[C_{14}mim][Phe]$ (**Fig. 1.30**) in aqueous solutions [72]. Surface tension and electrical conductivity measurements were utilized to evaluate their aggregation tendencies. Surface tension measurements revealed that $[C_{14}mim][Phe]$ has the lowest CMC and surface tension, which can arise due to the interaction between the aromatic ring of phenylalanine and the imidazole ring and the hydrophobicity of phenylalanine. The effect of temperature on the CMC values was examined through conductivity measurements and the results showed that the CMC values of three different AAILS increase with the temperature [72].

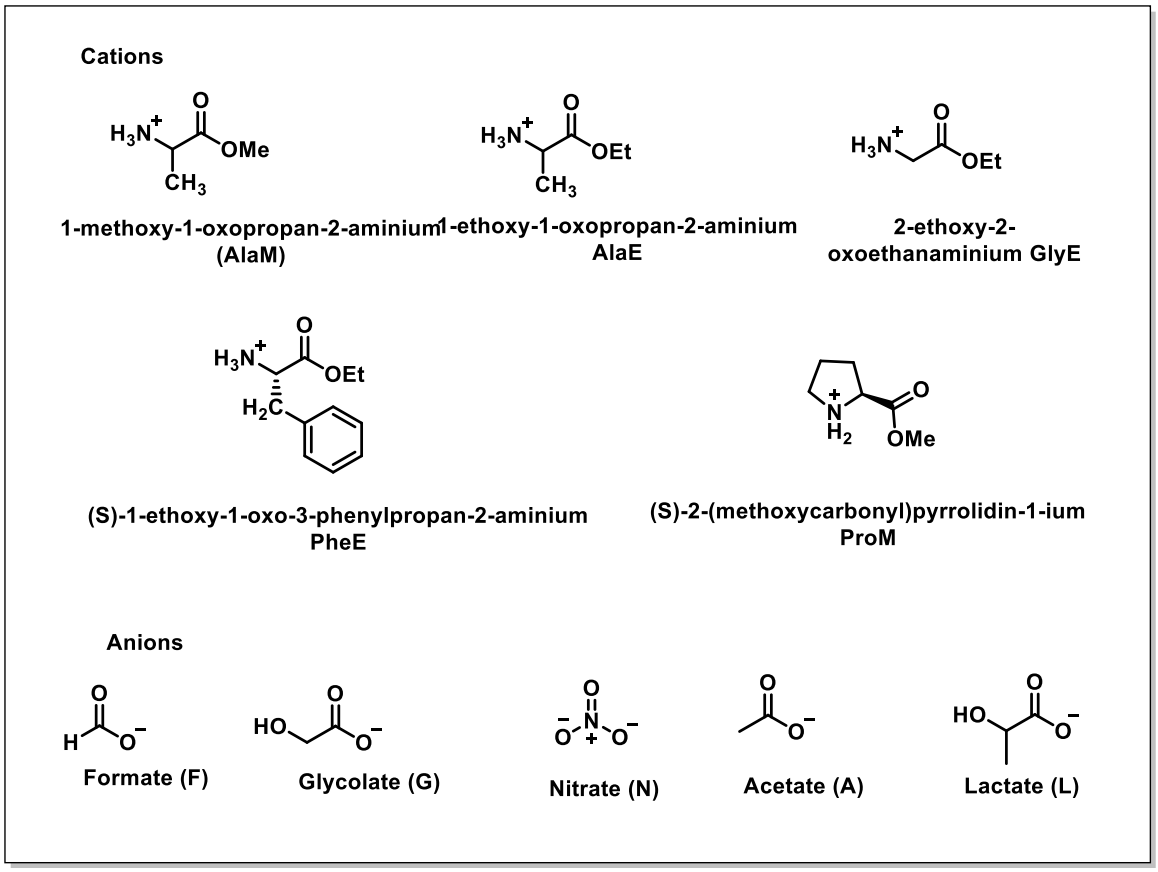

Fig.1.29: Structure of the cations and anions used in the AAILs.

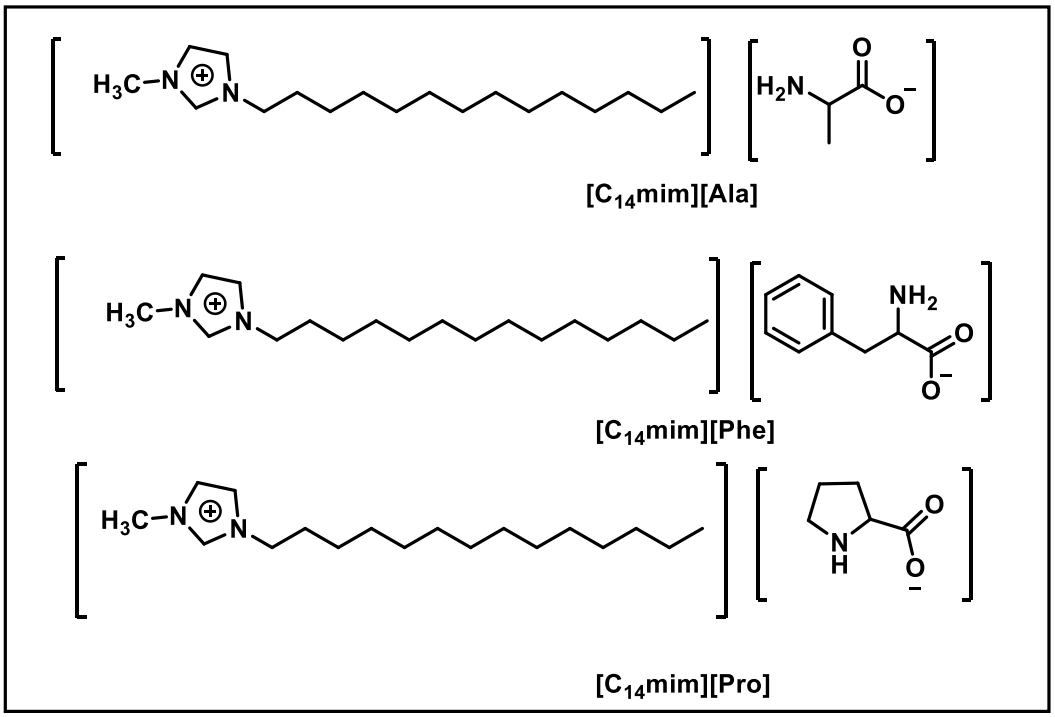

Fig. 1.30: Structure of the three AAILs.

Proper evaluation of the physicochemical properties of the ILs, have proven to be beneficial in identification of their applications as solvents, electrolytes, catalyst, etc. A proper investigation of the physicochemical properties of physicochemical properties of the room-temperature acidic ionic liquids (RTAILs) involves considering the effect of the constituent ion-pairs, the chain length of their alkyl substituents, the nature of the available acidic sites, temperature and added solvents. Although, RTAILs were originally developed as alternative green solvent/reaction media, however, today they have been utilized in diverse fields owing to their fascinating physicochemical properties.

1.3 Application of ionic liquids in catalysis and nanoparticle synthesis

With the growing importance for development of sustainable processes in organic synthesis, the task specific ionic liquid materials like acidic ILs, basic ILs, halometallates etc. have been exploited as reusable green catalysts for several organic transformations [2, 26, 73-77]. Their high thermal stability, negligible vapour pressure, acidity, solubility in a vast range of solvents as well as easy recyclability make them suitable candidates for catalysts in various organic transformations. Further, the growth of task-specific acidic or basic ionic liquids has shown significant contribution as dual-functionalized solvent-catalyst systems in organic reactions [26, 73-75]. These ILs have the potential to replace traditional non-recyclable mineral acids, bases, and Lewis-acid catalysts in organic syntheses. The first part of this section (**sub-section 1.3.1**) includes a brief discussion on catalytic applications of the ILs in Claisen-Schmidt condensation, Michael-like addition, and synthesis of 2-amino-3-cyanopyridines.

The utilization of the ILs is however not limited to catalysis alone. Recent years have reported their potential uses in nanoparticle synthesis [16, 18, 78-82]. The nanoparticles specially transition metal nanoparticles have garnered particular attention from industries and researchers alike, owing to their multiple fascinating properties like large surface area, lower melting points, specific magnetization, high mechanical strength and specific optical properties [18]. The metallic nanoparticles have found numerous industrial and biological applications such as catalysis, fuel cells, batteries, drug delivery, sensor and biosensors [82-87]. Due to the growing significance of metal nanoparticles in almost all the branches of science and technology, the researchers are focused on developing greener methods for their synthesis. In this regard the use of ILs in nanoparticle synthesis

has received considerable attention from the researchers. The inherent amphiphilicity of the ILs due to the presence of distinct hydrophilic and hydrophobic molecular fragments **(Fig. 1.27)** makes them display characteristics similar to classical surfactants. This surfactant-like property of the ILs along with the existence of H-bonding interactions, large number of charge carriers and tunable polarity, have been utilized successfully in their applications as solvents/capping agents for the preparation of a variety of nanoparticles including quantum dots (QDs) [13, 79, 81-84, 88, 89]. There also exist a few reports on the preparation and characterization of metal nanoparticles or QDs employing ILs as precursors or templates [16, 90-93]. Sub-section **1.3.2** gives an elaborate description of the applications of ILs in nanoparticle synthesis.

1.3.1 Catalytic application of ILs

This section highlights the applications of target specific ILs as solvent/catalyst system in Claisen-Schmidt condensation, Michael-like addition, and synthesis of 2-amino-3-cyanopyridines pyridines.

1.3.1.1 Claisen-Schmidt condensation

The Claisen-Schmidt condensation of aromatic aldehydes with ketones yields a class of α, β- unsaturated aromatic ketones known as 'chalcones'. Chalcones are readily available in nature as the core unit in variety of biologically active molecules with antibacterial, antifungal, antimalarial, antiviral, antioxidant, anti-inflammatory, antituberculosis and anticancer properties [94-97]. Chalcones are also the naturally available precursors of flavonoids, isoflavonoids, pyrazoles, isoxazoles and thiazoles [98-100]. The traditional methods used in the synthesis of chalcones employed strong acidic or basic reagents/catalysts like NaOH, $Ba(OH)_2$, KOH, $AlCl_3$ and HCl,[100] which often had the drawbacks of catalyst recovery, lower product selectivity, longer reaction time, extreme reaction conditions and tedious isolation process. Thus, to overcome these shortcomings, several methodologies for greener synthesis of chalcones have been observed in recent years. Many of these new green methodologies have employed ionic liquids as catalysts/solvents.

Shen et.al. synthesized chalcones via Claisen Schmidt condensation between benzaldehyde and acetophenone, catalysed by $–SO_3H$ functionalized imidazolium based ionic liquids (**Scheme 1.1)** [101]. The ILs played the dual role of solvent and catalyst and

produced chalcones at high yields (94-97%). Among these ILs, [(HSO_3)BBIM][HSO_4] **(Fig. 1.31A)** showed the best catalytic activity with a shorter reaction time[101].

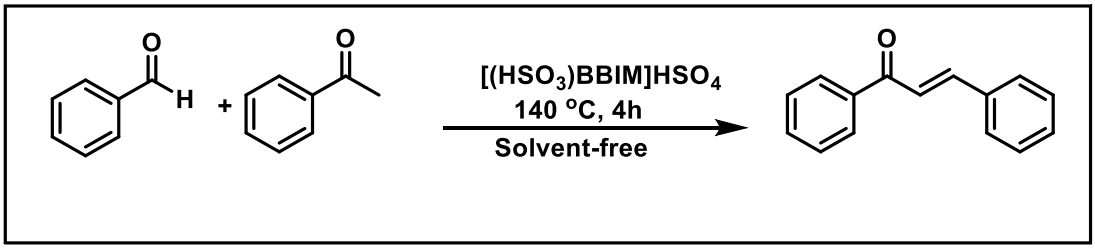

Scheme 1.1: Claisen-Schmidt condensation catalyzed by [(HSO_3)BBIM] [HSO_4].

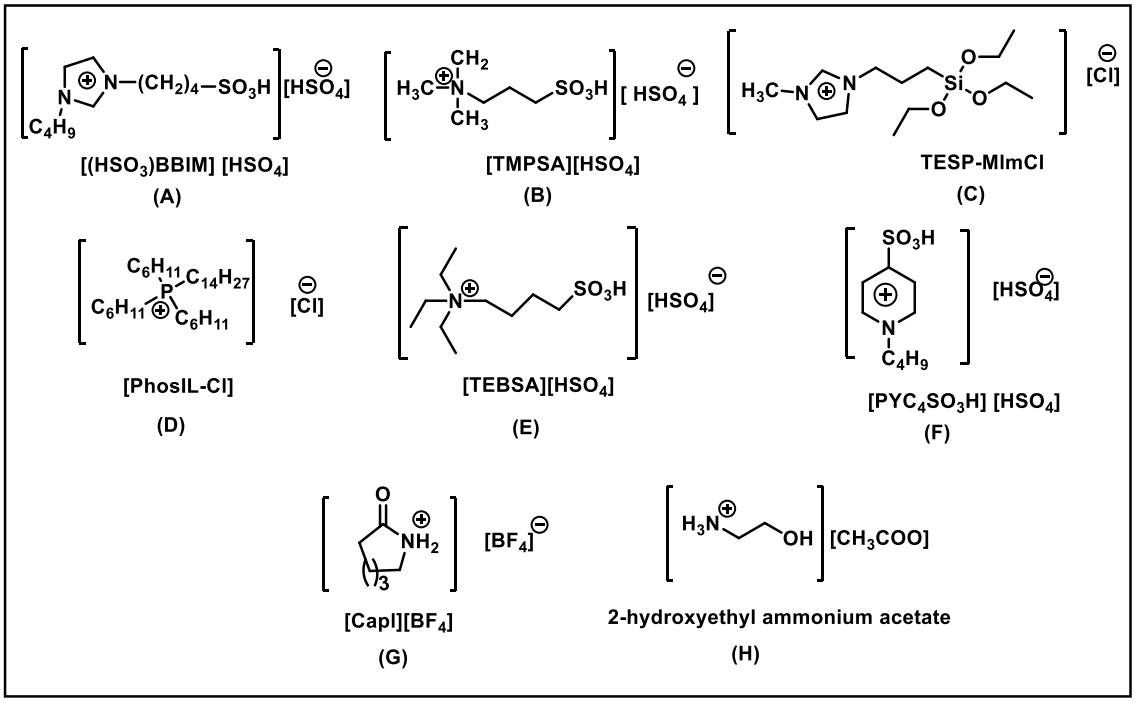

Fig. 1.31: Structures of the ILs used to catalyze Claisen-Schmidt condensation.

Dong et al. developed five reusable task-specific ionic liquids containing an alkanesulfonic acid group in an acyclic trialkylammonium cation for catalyzing the Claisen-Schmidt condensation [102]. Among the five TSILs, [TMPSA][HSO_4] (**Fig. 1.31B**) was identified as the best catalyst. The other four TSILs had comparatively longer alkyl chains that decrease their acidity by +I inductive effect. The lower acidity of the four ILs decreased their catalytic performance compared to [TMPSA][HSO_4]. 20 mol% [TMPSA][HSO_4] was sufficient to get excellent yields (>90%) of chalcones in a 2h reaction at 140 °C under nitrogen atmosphere **(Scheme 1.2)** [102].

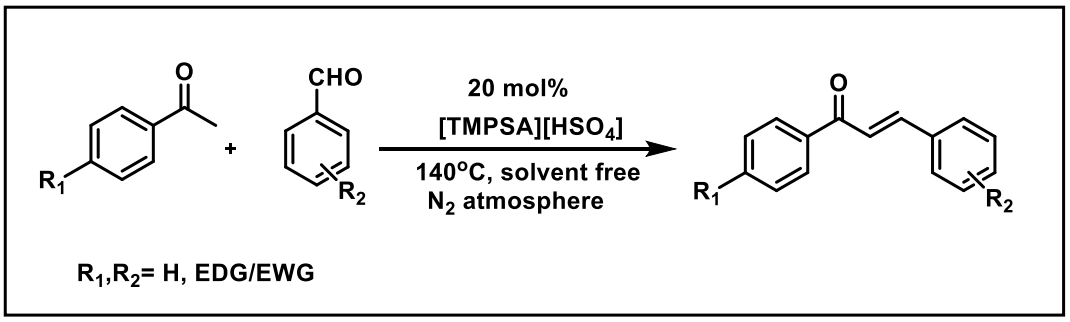

Scheme 1.2: Claisen-Schmidt condensation catalyzed by [TMPSA][HSO_4].

Kunde et.al. reported the synthesis of chalcones via Claisen-Schmidt condensation between 2′- hydroxyl acetophenone and benzaldehyde catalyzed by ionic liquid 1-(tri-ethoxy-silyl-propyl)-3-methylimidazolium chloride (TESP-MlmCl) (**Fig. 1.31C**) coated Zn-Al hydrotalcites (**Scheme 1.3)** [103]. The synthesized chalcones then underwent cyclisation to form flavonones.

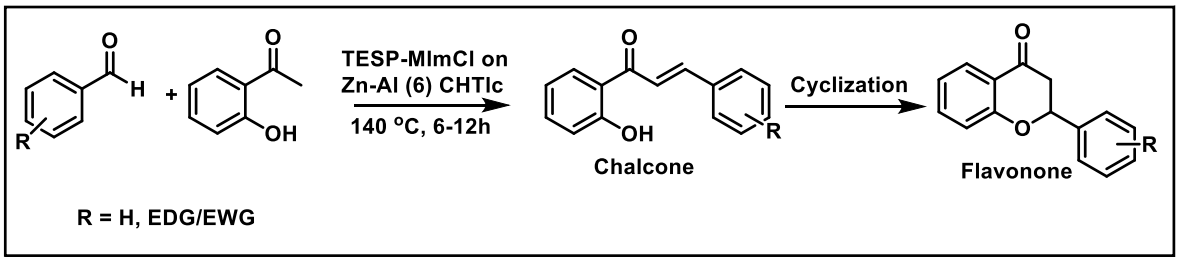

Scheme 1.3: Claisen-Schmidt condensation catalyzed by (TESP-MlmCl) coated Zn-Al hydrotalcites.

Sarda et al. synthesized chalcones via Claisen-Schmidt condensation reaction catalyzed by a phosphonium based ionic liquid tetradecyl-(trihexyl)-phosphonium chloride [PhosIL-Cl] (**Fig. 1.31D**) [104]. The products were obtained with 90% yield at in 3 hours reaction time at 70°C (**Scheme 1.4)** [104**]**.

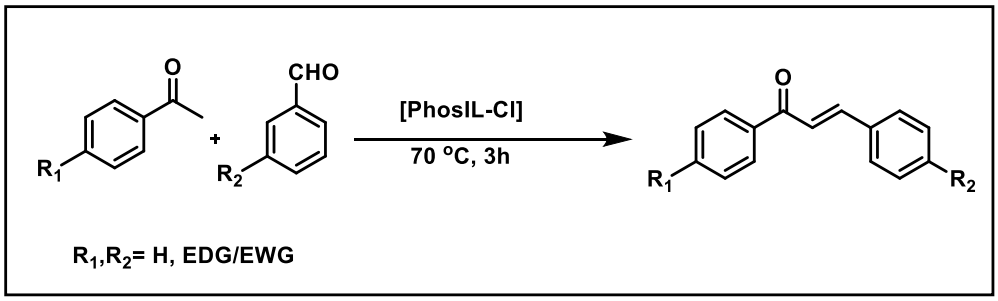

Scheme 1.4: Claisen-Schmidt condensation catalyzed by [PhosIL-Cl].

Pan et al. developed a microwave-assisted liquid phase synthesis of amino chalcones using aldehyde-functionalized ionic liquid as soluble support **(Scheme 1.5)** [105]. 4-aminoacetophenone binds with the aldehyde-functionalized ionic liquid. This ionic liquid bound aminoacetophenone was then treated with aromatic aldehyde to give supported chalcone derivatives, which were then efficiently cleaved from the support. The products were obtained with high yields (87-92%) [105].

Qian et al., developed a series of N,N,N-triethyl-N-butanesulfonic acid ammonium ILs [TEBSA][X] (where X= HSO_4, NO_3, CF_3COO, p-TSO) as catalysts for the Claisen-Schmidt condensation of aromatic aldehyde with acetophenone [106]. [TEBSA][HSO_4] (**Fig. 1.31E**) was found to be the most acidic IL and hence, was identified as the best catalyst for the given reaction. This condensation reaction utilised 20 mol% of [TEBSA][HSO_4] catalyst at 120°C, under nitrogen atmosphere to give 84–95% yield of the product in 2-4 hours **(Scheme 1.6)** [106].

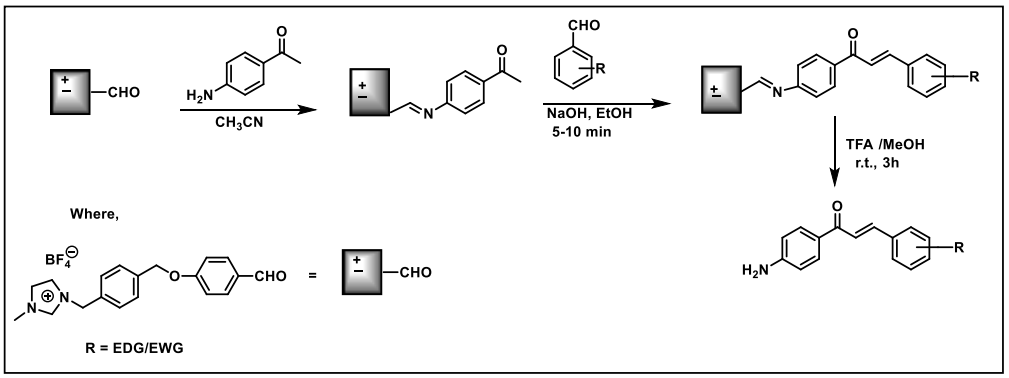

Scheme 1.5: Claisen-Schmidt condensation catalyzed by aldehyde-functionalized ionic liquid.

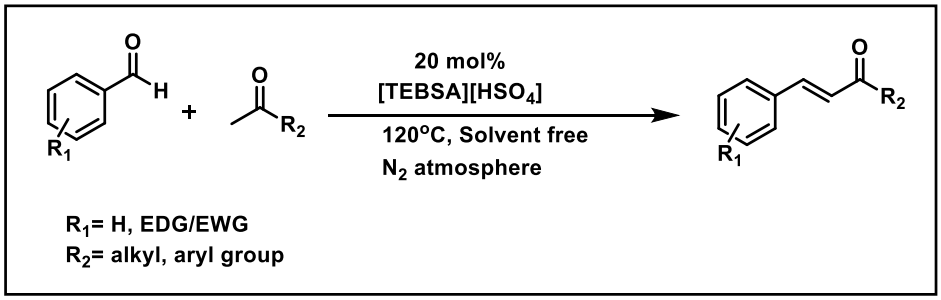

Scheme 1.6: Claisen-Schmidt condensation catalyzed by [TEBSA][HSO_4].

Davoodnia et.al. developed a new solid acidic catalyst by impregnating silica (Aerosil 300) with ionic liquid 1-(4-sulfonic acid) butylpyridinium hydrogen sulphate [PYC_4SO_3H] [HSO_4] (**Fig. 1.31F**) [107]. This reusable heterogeneous catalyst designated [PYC_4SO_3H] [HSO_4]/A300SiO_2 was used with high efficiency to catalyze

Claisen-Schmidt condensations between ketones and aromatic aldehydes **(Scheme 1.7)** leading to the formation of chalcones and cycloalkanones [107].

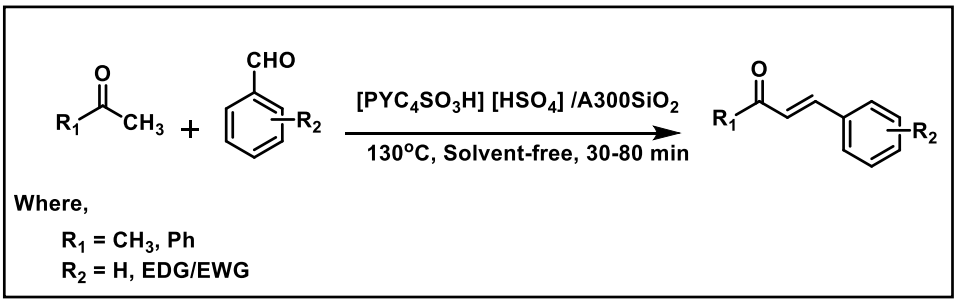

Scheme 1.7: Claisen-Schmidt condensation catalyzed by [PYC_4SO_3H] [HSO_4] /A300SiO_2.

Qian et al. carried out the Claisen−Schmidt condensation of 2'-hydroxyacetophenone with benzaldehyde using a series of caprolactam-based ionic liquids ([Capl][X] where X= $CF_3CO_2^-$, BF_4^-, NO_3^-, BSO^-) [108]. Among the four ILs [Capl][BF_4] (**Fig. 1.31G**) was found to exhibit highest acidity and showed the best catalytic activity with 89% yield of 2'-hydroxychalcone under ultrasonic irradiation **(Scheme 1.8)** [108].

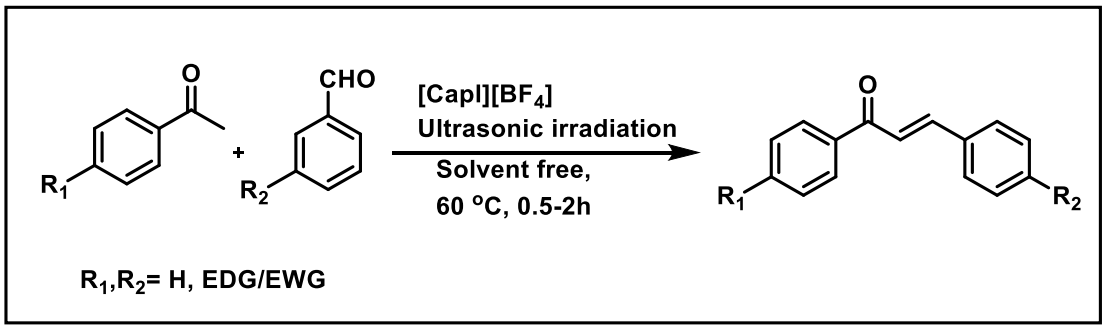

Scheme 1.8: Claisen-Schmidt condensation catalyzed by [Capl][BF_4].

Xiaoyun et.al. used an ionic liquid 2-hydroxyethyl ammonium acetate (**Fig. 1.31F**) as a catalyst for Claisen-Schmidt condensation between acetophenone and aromatic aldehydes to prepare chalcones under solvent-free conditions **(Scheme 1.9).** The ionic liquid showed good catalytic activity and recyclability [109].

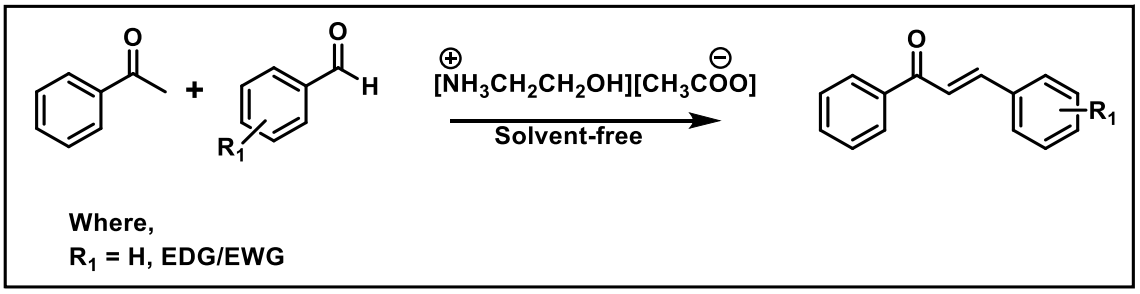

Scheme 1.9: Claisen-Schmidt condensation catalyzed by [$^+NH_3CH_2CH_2OH$][CH_3COO^-].

1.3.1.2 Michael addition

Michael additions are a common organic C-C bond formation reaction where nucleophilic addition of a carbanion or another nucleophile to an α, β-unsaturated carbonyl compound occurs. In this section, we will mostly focus on the preparation of 3-substituted indoles via Michael-like addition of indole to α, β-unsaturated carbonyl compounds. These 3-substituted indoles are found amply in nature as flower scents, perfumes as well as in coal tar. They are known to possess antifungal, antimicrobial, antiviral, anti-inflammatory and analgesic activities [110, 111]. The primary preparation route of 3- substituted indoles involves Michael-like addition reaction of indole with α, β-unsaturated ketones using either Brønsted or Lewis acid catalysts [111-117]. Some of the reactions require a careful control of acidity to prevent side reactions such as dimerization or polymerization. Further, most of these processes involve tedious chromatographic separation of products, lower yields, longer reaction time and less product selectivity. With the growing significance of 3-substituted indoles, several environmentally sustainable and effective methodologies have been developed for their synthesis. Some of these reports involve using ionic liquids as catalysts or solvent.

Gu et al. used an acidic IL 1-N-hexyl-3-methylimidazolium hydrogen sulfate [hMIM][HSO_4] **(Fig. 1.32A)** as a recyclable catalyst for the Michael addition of indoles to α, β-unsaturated ketones (**Scheme 1.10)** [118]. The use of 10 mol% of [hMIM][HSO_4] catalyst in ethanol produced β-indolylketones with 99% yield.

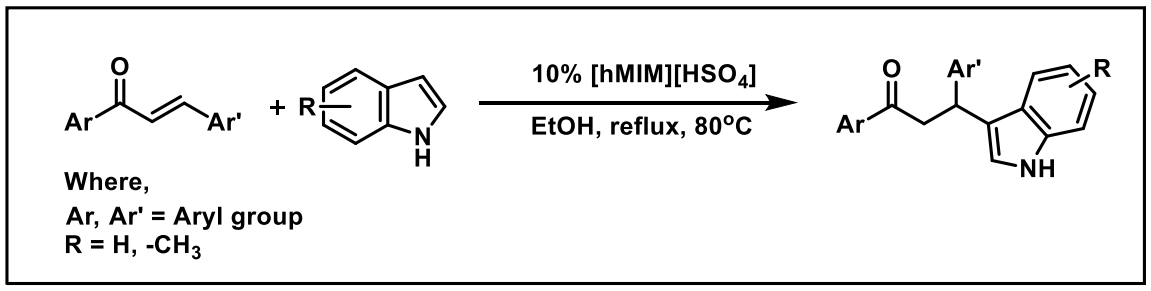

Scheme 1.10: Michael addition of indoles to α,β-unsaturated ketones catalysed by [hMIM][HSO_4].

Liu and co-workers reported a N-alkyl –SO_3H functionalized pyridinium cation based BAIL [$PyN(CH_2)_4SO_3H$][*p*-CH_3PhSO_3] **(Fig. 1.32B)** as an efficient catalyst in acetonitrile for the preparation of β-indolyl ketones (**Scheme 1.11)** [119]. The products

were obtained at higher yields (74-97%) and the catalyst exhibited good recyclability [119].

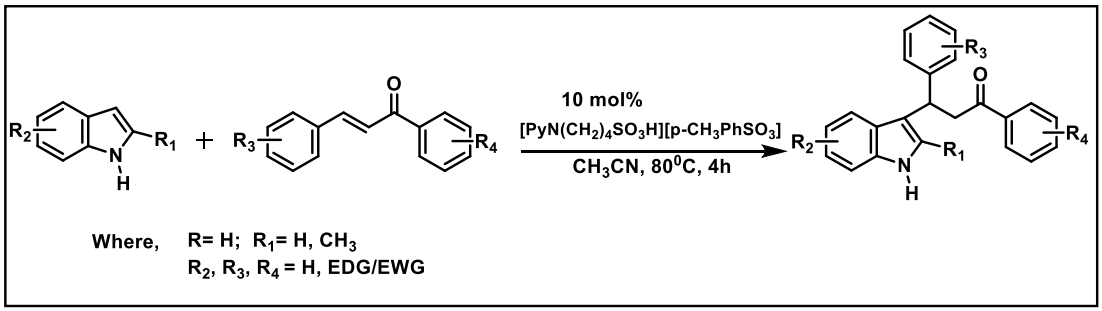

Scheme 1.11: Michael addition of indoles to chalcones catalysed by a BAIL.

The same group later carried out the Michael addition reaction of indoles with α, β-unsaturated ketones (**Scheme 1.12A & B)** using the BAILs [PSbbim][p-CH_3PhSO_3] **(Fig. 1.32 C)** [120] and [ThiN(CH_2)4SO_3][p-CH_3PhSO_3] **(Fig. 1.32 D)** [121]. In both the cases, the BAIL catalyst was successfully recycled up to three times and the products were obtained at high yields (85-99%) [120,121].

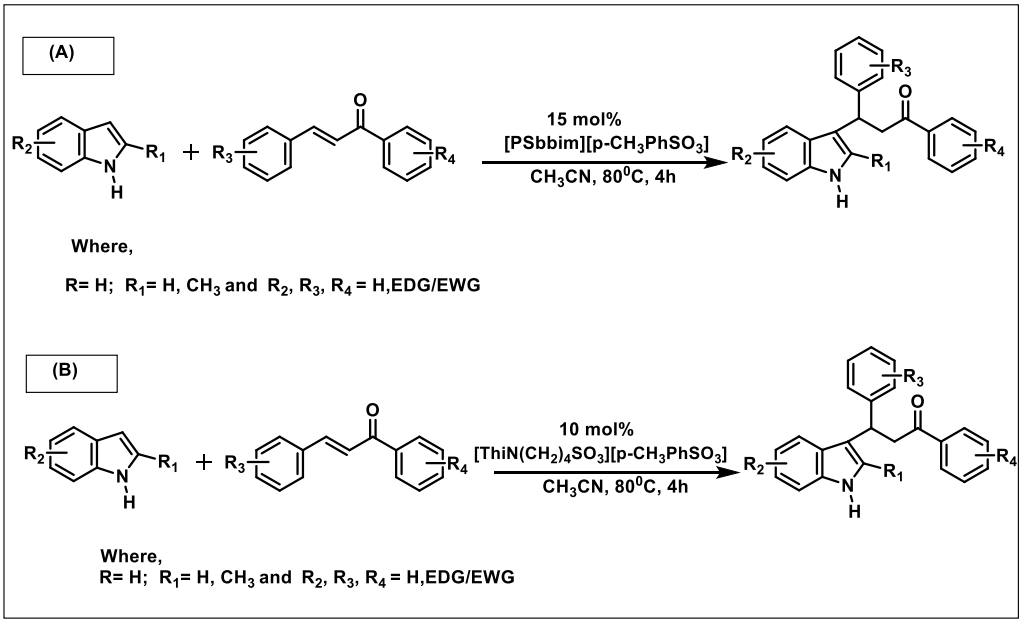

Scheme 1.12: Michael addition of indoles to chalcones catalysed by **(A)** [PSbbim][p-CH_3PhSO_3] **(B)** [ThiN(CH_2)4SO_3][p-CH_3PhSO_3].

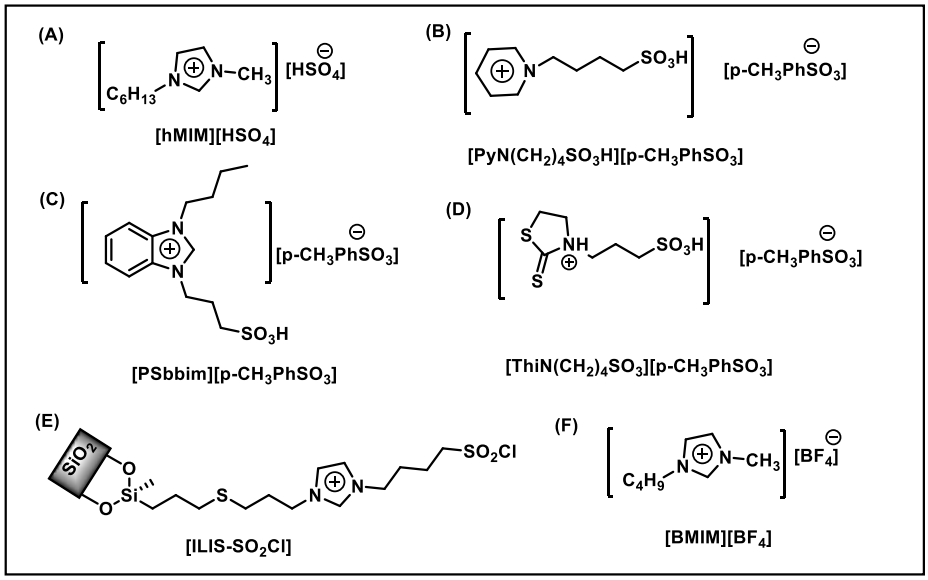

Fig. 1.32: Structures of the ILs used to catalyze Michael addition of indole.

Hagiwara et al. developed a new efficient and mild method for the 1,4-conjugate addition of indoles to vinyl ketones employing a Lewis acidic ionic liquid (LAIL) immobilized on silica (ILIS-SO_2Cl) **(Fig. 1.32E)** as a catalyst (**Scheme 1.13)** [122]. The catalyst was recycled up to six times and products were obtained with high yield (72-92%) [122].

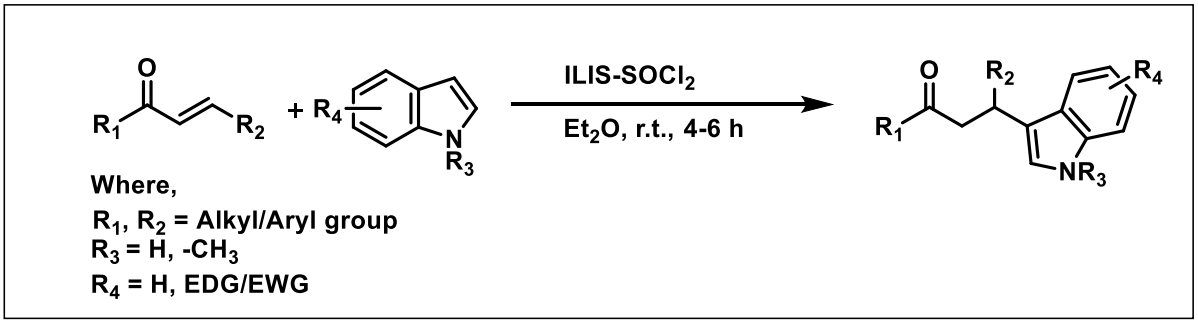

Scheme 1.13: Michael addition of indoles to α,β-unsaturated ketones catalysed by LAIL immobilized on silica (ILIS-SO_2Cl).

Apart from being used as a catalyst, the ILs were also used as solvents in Michael addition reactions. Yadav et al. found that treatment of indole with α, β-unsaturated ketones in the presence of 10 mo1% copper (II) triflate immobilized in IL [BMIM][BF_4] **(Fig. 1.32F)** resulted in the formation of Michael adduct in high yields (85-95%) **(Scheme 1.14A)** [123]. Li et al. utilised the same IL as a solvent for $PdCl_2(CH_3CN)_2$ catalyzed Michael addition reaction of indoles with α, β-unsaturated ketones **(Scheme 1.14B)** [124].

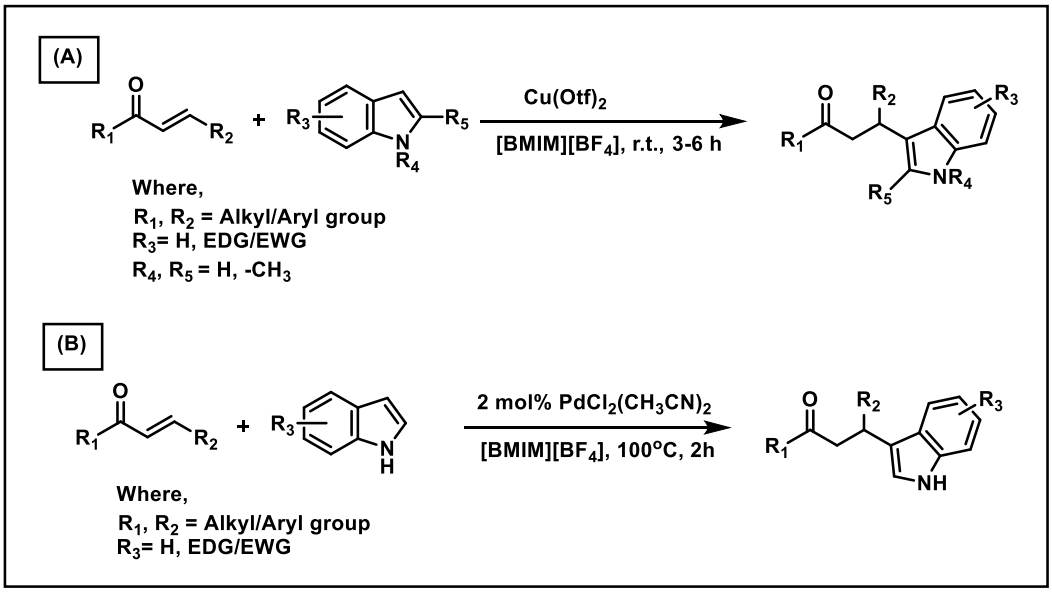

Scheme 1.14: Michael addition of indoles to α, β-unsaturated ketones using IL [BMIM][BF_4] as a solvent and (A) $Cu(OTf)_2$ and (B) $PdCl_2(CH_3CN)_2$ as catalyst.

1.3.1.3 Multicomponent synthesis of 2-amino-3-cyanopyridines

Multicomponent "one pot" synthesis is an attractive greener approach for reactions of three or more reactant molecules in one reaction vessel to give the desired product selectively, without isolation of any reaction intermediate involved in the different steps [29]. These type of reaction tries to minimise the overall reaction time and laborious purification techniques. ILs have proven to be efficient catalysts for several multicomponent reactions like Mannich reaction, Biginelli reaction, synthesis of heterocycles etc. This sub-section includes the up-to-date literature for IL catalysed multicomponent synthesis of 2-amino-3-cyanopyridines. As a heterocyclic compounds, the 2-amino-3-cyanopyridines exhibit a diverse array of biological activities including anti-bacterial activity [125], HIV-1 integrase inhibition, anti-parkinsonism [126], IKK-β inhibition [127], A_{2A} adenosine receptor antagonistic properties [128], carbonic anhydrase inhibition [129], antifungal [130], anti-inflammatory [127], anticancer properties [131] etc. Hence, greener methods for their synthesis using ionic liquids have gained prominence over the years.

Sarda et al. employed chalcones for condensation with malononitrile and ammonium acetate in the presence of ionic liquid ethylammonium nitrate ([$EtNH_3$][NO_3]) **(Fig. 1.33A)** to synthesize 2-amino-3-cyanopyridines in high yields (80-90%) and shorter time **(Scheme 1.15)**. The IL was recycled up to three times [132].

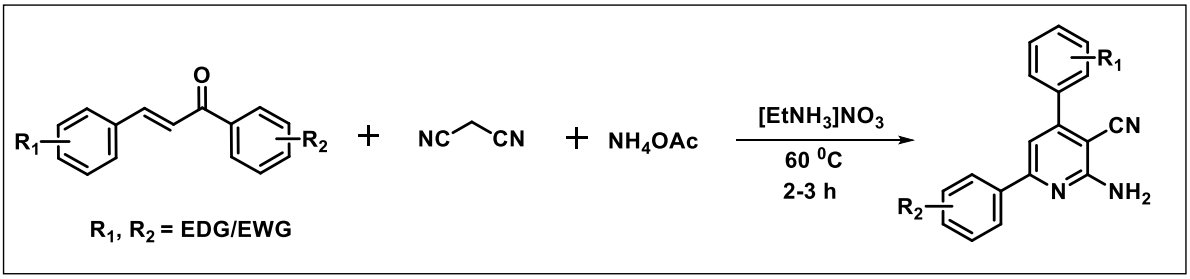

Scheme 1.15: Multicomponent synthesis of 2-amino-3-cyanopyridines catalysed by $[EtNH_3][NO_3]$.

Wan et al. synthesized aryl-substituted 2-amino-4-aryl-5,6,7,8-tetrahydroquinoline-3-carbonitriles via a four-component one-pot reaction of aromatic aldehyde, cyclohexanone, malononitrile, and amines in basic ionic liquid [BMIM][OH] **(Fig. 1.33B)** with good yields (70-86%) **(Scheme 1.16)** [133].

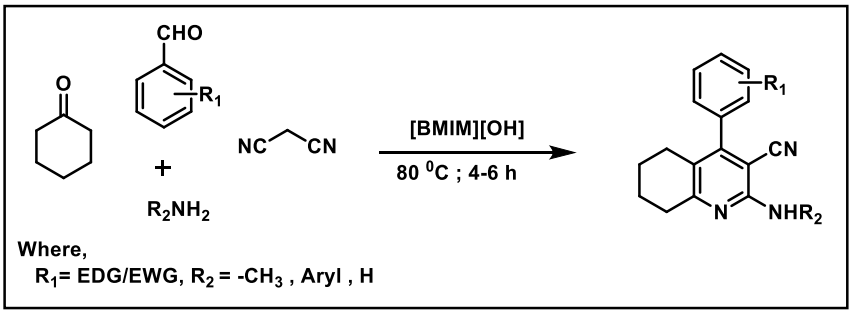

Scheme 1.16: Multicomponent synthesis of 2-amino-4-aryl-5,6,7,8-tetrahydroquinoline-3-carbonitriles catalysed by [BMIM][OH].

Mansoor and his group employed 1-butyl-3-methylimidazolium tetrafluoroborate ($[BMIM][BF_4]$) **(Fig. 1.32F)** ionic liquid as a solvent-catalyst system for the multicomponent preparation of 2-amino-3-cyanopyridine derivatives **(Scheme 1.17)**. Shorter reaction time, high yields (78-92%) and environmentally sustainable conditions were the advantages of the above method [134].

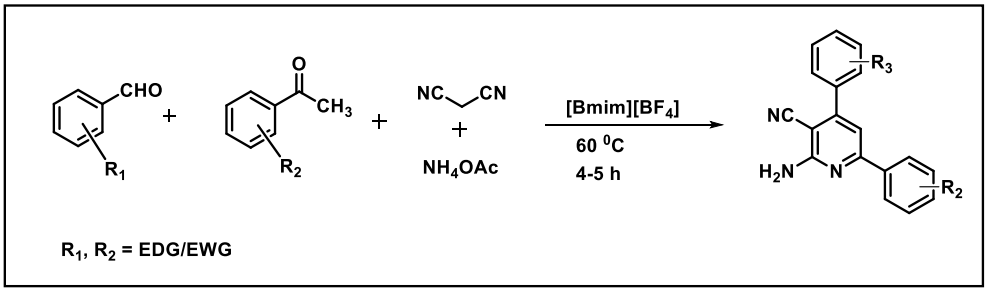

Scheme 1.17: Multicomponent synthesis of 2-amino-3-cyanopyridines catalysed by [BMIM][BF_4].

Tamaddon et al. utilized a nicotine based protic ionic liquid (PIL), nicotinum methane sulfonate (NMS) **(Fig. 1.33C)** for the synthesis of 2-amino-3-cyanopyridines under solvent free conditions **(Scheme 1.18)** [135]. The products were obtained at high yields (78-98%) and the catalyst was recycled up to 3 times.

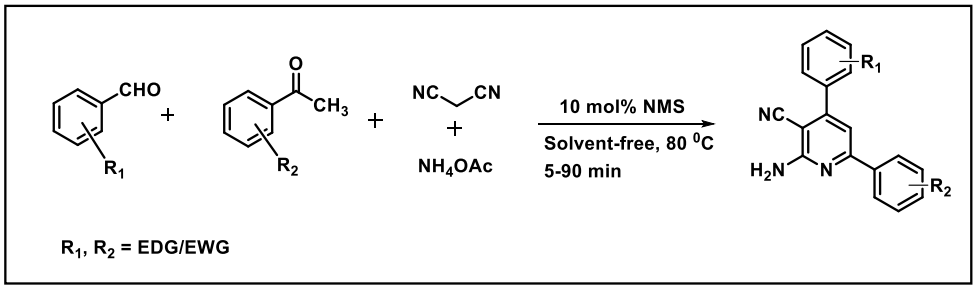

Scheme 1.18: Multicomponent synthesis of 2-amino-3-cyanopyridines catalysed by NMS.

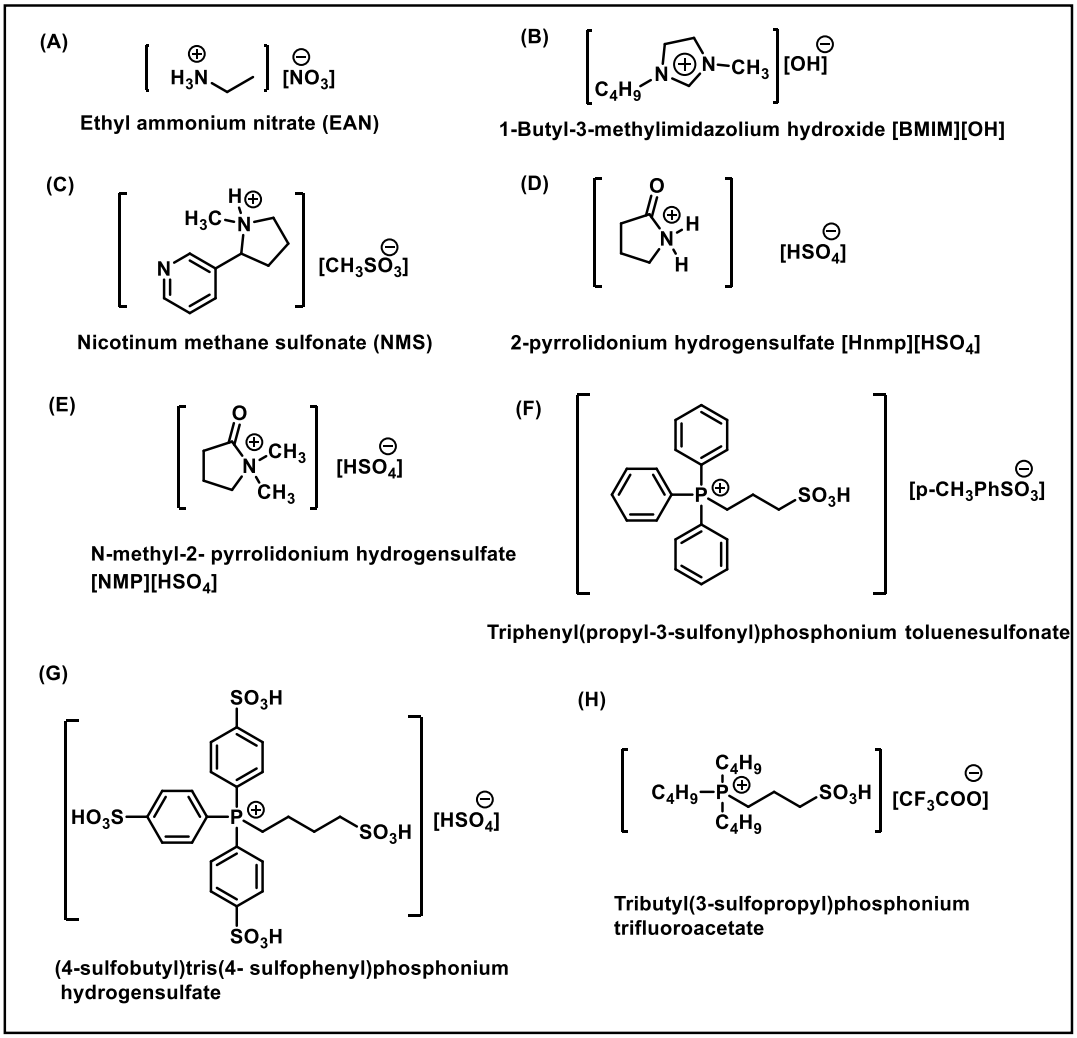

Fig. 1.33: Structures of the ILs used in multicomponent synthesis of 2-amino-3-cyanopyridines.

Mollashahi et al. used four BAILs 2-pyrrolidonium hydrogensulfate ([Hnmp][HSO_4]), N-methyl-2-pyrrolidonium hydrogensulfate ([NMP][HSO_4]), triphenyl(propyl-3-sulphonyl)phosphonium toluenesulfonate and (4-sulfobutyl)tris(4-sulfophenyl)phosphonium hydrogensulfate **(Fig. 1.33 D-G)** as catalysts one-pot four-component condensation between aromatic aldehydes, substituted acetophenones, malononitrile and ammonium acetate to afford corresponding 2-amino-3- cyanopyridine derivatives **(Scheme 1.19)** [136]. All the four BAILs displayed similar catalytic activity. 30 mol% of the BAILs gave products with 92-95% yields within 5-7 minutes [136].

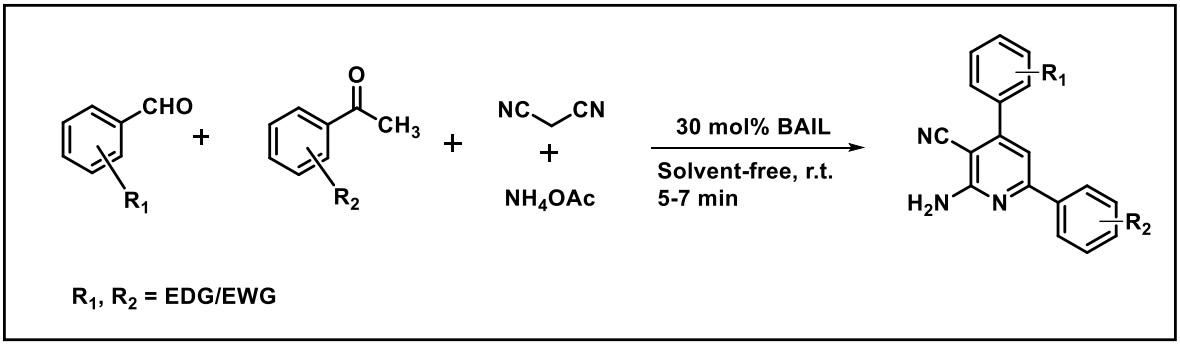

Scheme 1.19: Multicomponent synthesis of 2-amino-3-cyanopyridines catalysed by BAILs.

Zolfigol and co-workers designed a phosphonium based BAIL tributyl(3-sulfopropyl)phosphonium trifluoroacetate **(Fig. 1.33H)** as a catalyst for the synthesis of 2-amino-3-cyanopyridines **(Scheme 1.20)**. The reaction was carried out in presence of 10 mol% of catalyst under solvent-free conditions at 80°C and the products were obtained at high yields (75-90%) [137].

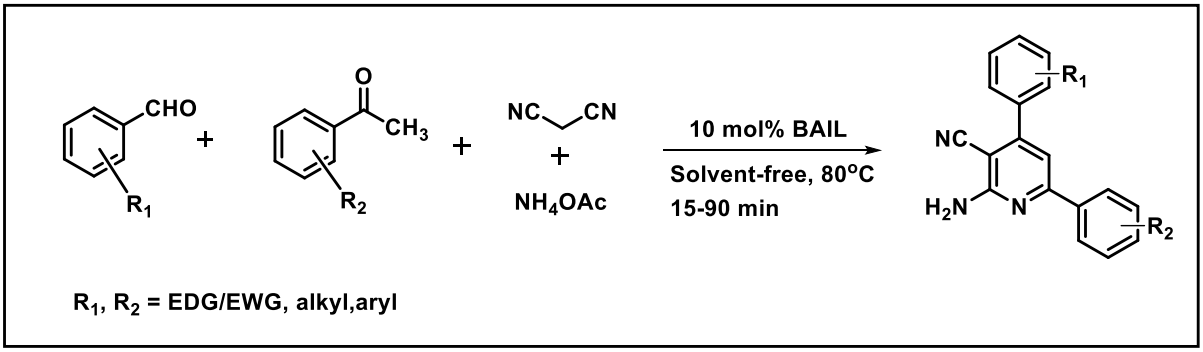

Scheme 1.20: Multicomponent synthesis of 2-amino-3-cyanopyridines catalysed by a phosphonium based BAIL.

1.3.2 Application of ILs in nanoparticle synthesis

Over the years, the ILs have found several applications in nanotechnology. The synthesis of metal nanoparticles primarily in ionic liquids as a media/template/precursor has attained consideration due to mono-dispersive and non-agglomerative behaviours of the nanoparticles in them [18]. The cations and/or anions of the ILs stabilize these nanoparticles preventing their agglomeration. The cations and anions of the ILs are known to form an electrical double layer surrounding the nanoparticles to keep the nanoparticles away from one another and thus, preventing their aggregation. Apart from the electrostatic interactions, the van der Waals and hydrogen bonding interactions along with the structure, solvophobicity and steric factors also play significant roles in stabilizing the metal nanoparticles in ILs. These factors are also responsible for controlling their morphology and particle size of the metal nanoparticles. The size distribution of the metal nanoparticles is significantly affected by the nature and degree of ionic liquid-nanoparticle interactions, which in turn are dependent on the nature of the constituent ions and the physiochemical properties of the ionic liquids [138, 139]. For instance, ILs having longer side chains are responsible for the smaller diameter and narrower distributions of metal nanoparticles [138]. The formation of larger sized nanoparticles can be observed in ILs with smaller anions and can be attributed to the agglomeration of the unstable metallic nanoparticles through strong coulombic forces of attraction [138, 140]. Furthermore, the decreased viscosity of the ILs at elevated temperatures causes the rapid diffusion of metal nanoparticles leading them to form aggregates and thus resulting in larger nanoparticles [141].

As already mentioned earlier, the ILs have been successfully utilized as solvents and capping agents in synthesis of nanoparticles [18, 78, 79, 80, 89, 138, 139, 142-144]. Apart from their use as solvent or capping agent in nanoparticle synthesis, there exist a few reports where the ILs, especially the metal containing halometallate ILs, have also been utilised as precursors/templates for nanoparticle synthesis. Iida et al. synthesized silver nanoparticles from Ag based ILs $[Ag(eth\text{-}hex\text{-}en)_2][NO_3]$ and $[Ag\text{-}(hex\text{-}en)_2][PF_6]$ **(Fig. 1.34 A & B)** by treatment with aqueous $NaBH_4$ [91].

Liu et al. used a Se-containing ionic liquid 1-n-butyl-3-methylimidazolium methylselenite ($[BMIm][SeO_2(OCH_3)]$) **(Fig. 1.34 C)** as a Se precursor to synthesize

ZnSe hollow nanospheres through a one-pot hydrothermal method [24]. The synthesized ZnSe hollow nanospheres had an average diameter of about 100 nm and a wall thickness of about 10-20 nm. It was found that [BMIm][$SeO_2(OCH_3)$] served both as Se source and a stabilizer for the ZnSe hollow nanospheres [92].

Xu et al. synthesized α-Fe_2O_3 nano cubes employing iron containing chlorometallate IL [$(C_8H_{17})_2(CH_3)_2N$][$FeCl_4$] and water at liquid/liquid interface using hydrothermal method **(Fig. 1.34D)** [90].

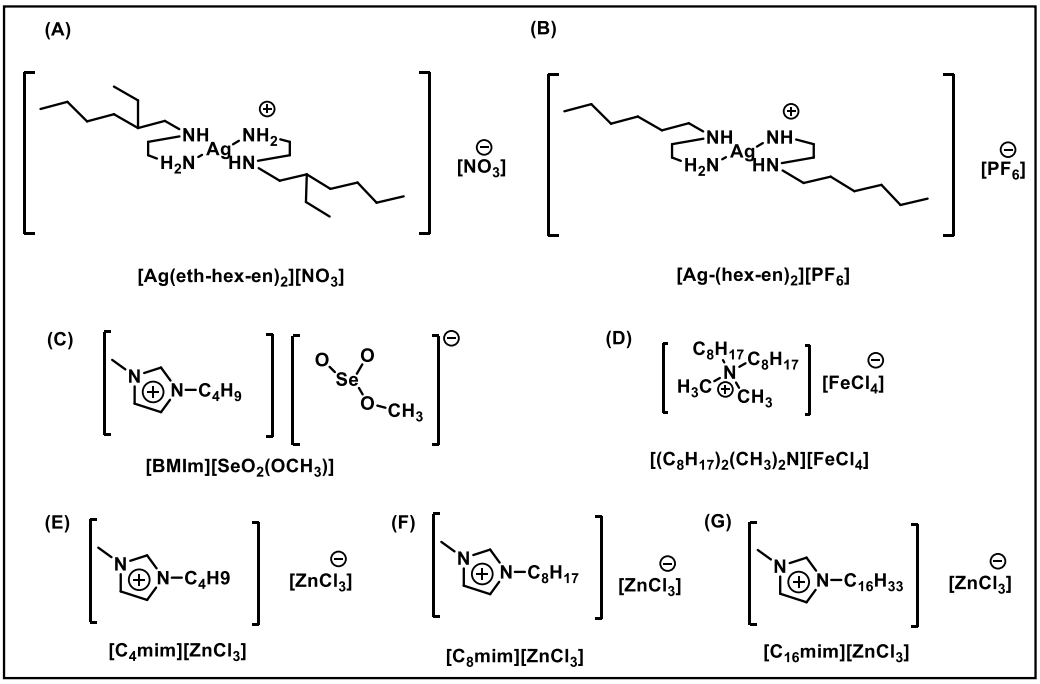

Fig.1.34: Structures of the ILs used as precursors in metal nanoparticle synthesis.

Komal et al. developed an economical and greener method for preparation of Zinc Sulphide (ZnS) quantum dots, where zinc (metal M) containing ionic liquids (MILs), [$C_n$mim][$ZnCl_3$], (Where, n = 4, 8, 16**) (Fig. 1.34 E-G)** have been used as precursor, template as well as solvent **(Scheme 1.21)** [16]. ZnS (QDs) were synthesized at room temperature by a simple grinding method, where the zinc containing MILs were grinded with Na_2S. The spherical ZnS QDs formed had an average diameter of 1.5-5.0 nm, which decreases with the increasing alkyl chain length of the MILs [16].

Arora et al. also synthesized ZnS-graphene nano-composites using a zinc-containing IL [C_{16}mim][$ZnCl_3$] **(Fig. 1.34G)** as a precursor/template for ZnS QDs. The process involves mixing the graphene with an aqueous solution of the IL, followed by the addition of Na_2S to obtain the ZnS-graphene nano-composites [144].

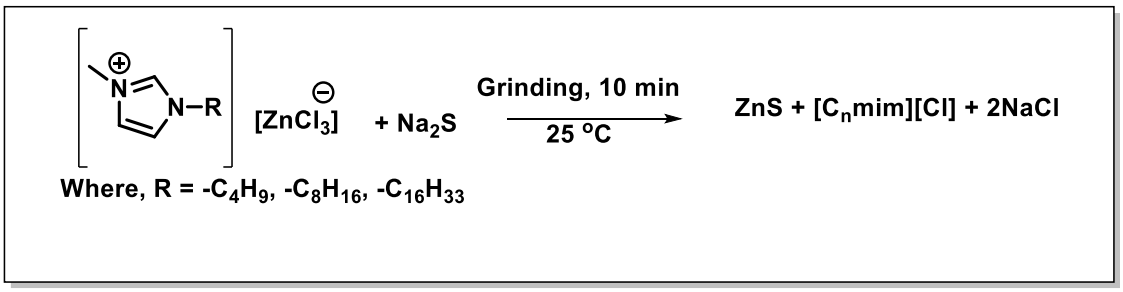

Scheme 1.21: Synthesis from ZnS QDs from MILs as precursor/template.

Thus, it can be seen that over the years, several methodologies have been successfully developed employing the use of ILs as solvents, capping agents, templates or even precursors in nanoparticle synthesis. As already mentioned earlier, the field of ionic liquids is ever-evolving and because of it, the applications of ILs are finding new dimensions every day.

Bibliography

[1] Anastas, P. T. and Williamson, T. C. *Green Chemistry: Theory and Practice*. Oxford University Press, USA, pages 29-56, 1998.

[2] Vafaeezadeh, M. and Alinezhad, H. Brønsted acidic ionic liquids: Green catalysts for essential organic reactions. *Journal of Molecular Liquids*, 218:95-105, 2016.

[3] Lei, Z., Chen, B., Koo, Y.M., and MacFarlane, D.R. Introduction: ionic liquids. *Chemical Reviews*, 117(10):6633-6635, 2017.

[4] Hawker, R. R. and Harper, J. B. Organic reaction outcomes in ionic liquids. In: Williams, I. H. and William, N. H., editors, *Advances in Physical Organic Chemistry*, volume 52, pages 49–79, ISBN: 978-0-12-815211-9. Elsevier, London, UK, 2018.

[5] Fei, Z., Geldbach, T.J., Zhao, D., and Dyson, P.J. From dysfunction to bis-function: on the design and applications of functionalised ionic liquids. *Chemistry–A European Journal*, 12(8):2122-2130, 2006.

[6] Zhang, S., Sun, N., He, X., Lu, X., and Zhang, X. Physical properties of ionic liquids: database and evaluation. *Journal of physical and chemical reference data*, 35(4):1475-1517, 2006.

[7] Olivier-Bourbigou, H., Magna, L., and Morvan, D. Ionic liquids and catalysis: Recent progress from knowledge to applications. *Applied Catalysis A: General*, 373(1-2):1-56, 2010.

[8] Maciejewski, H. Ionic liquids in Catalysis. *Catalysts*, 11(3):367, 2021.

[9] Dutta, A. K., Gogoi, P., Saikia, S., and Borah, R. N, N-disulfo-1, 1, 3, 3-tetramethylguanidinium carboxylate ionic liquids as reusable homogeneous catalysts for multicomponent synthesis of tetrahydrobenzo [a] xanthene and tetrahydrobenzo [a] acridine derivatives. *Journal of Molecular Liquids*, 225:585-591, 2017.

[10] Saikia, S. and Borah, R. One-pot sequential synthesis of 2-amino-4, 6-diaryl pyrimidines involving SO_3H-functionalized piperazinium-based dicationic ionic liquids as homogeneous catalysts. *ChemistrySelect*, 4(30):8751-8756, 2019.

[11] Vekariya, R. L. A review of ionic liquids: applications towards catalytic organic transformations. *Journal of Molecular Liquids*, 227:44-60, 2017.

[12] Ho, T.D., Zhang, C., Hantao, L.W., and Anderson, J.L. Ionic liquids in analytical chemistry: fundamentals, advances, and perspectives. *Analytical Chemistry*, 86(1):262-285, 2014.

[13] Trujillo-Rodríguez, M.J., Nan, H., Varona, M., Emaus, M.N., Souza, I.D., and Anderson, J.L. Advances of ionic liquids in analytical chemistry. *Analytical Chemistry*, 91(1):505-531, 2018..

[14] Zunita, M., Wahyuningrum, D., Bundjali, B., Wenten, I.G., and Boopathy, R. The performance of 1, 3-dipropyl-2-(2-propoxyphenyl)-4, 5-diphenylimidazolium iodide based ionic liquid for biomass conversion into levulinic acid and formic acid. *Bioresource Technology*, 315:123864, 2020.

[15] Xu, F., Sun, J., Konda, N. M., Shi, J., Dutta, T., Scown, C. D., Simmons, B. A., and Singh, S. Transforming biomass conversion with ionic liquids: process intensification and the development of a high-gravity, one-pot process for the production of cellulosic ethanol. *Energy & Environmental Science*, 9(3):1042-1049, 2016.

[16] Komal, Shikha, P., and Kang, T. S. Facile and green one pot synthesis of zinc sulphide quantum dots employing zinc-based ionic liquids and their photocatalytic activity. *New Journal of Chemistry*, 41(15):7407-7416, 2017.

[17] Gusain, R., Mungse, H. P., Kumar, N., Ravindran, T. R., Pandian, R., Sugimura, H., and Khatri, O.P. Covalently attached graphene–ionic liquid hybrid nanomaterials: synthesis, characterization and tribological application. *Journal of Materials Chemistry A*, 4(3):926-937, 2016.

[18] Verma, C., Ebenso, E. E., and Quraishi, M. A. Transition metal nanoparticles in ionic liquids: Synthesis and stabilization. Journal of Molecular Liquids, 276:826-849, 2019.

[19] Silvester D. S. Recent advances in the use of ionic liquids for electrochemical sensing. *Analyst.* 136:4871-4882, 2011.

[20] Paul, A., Muthukumar, S., and Prasad, S. Room-temperature ionic liquids for electrochemical application with special focus on gas sensors. *Journal of the Electrochemical Society*, 167(3):037511, 2019.

[21] Balducci, A. Ionic liquids in lithium-ion batteries. In Kirchner B and Perlt, E., editors, *Ionic Liquids II*, pages 1-27. Springer, 2018.

[22] Watanabe, M., Thomas, M.L., Zhang, S., Ueno, K., Yasuda, T., and Dokko, K. Application of ionic liquids to energy storage and conversion materials and devices. *Chemical reviews*, 117(10):7190-7239, 2017.

[23] Mallakpour, S. and Rafiee, Z. New developments in polymer science and technology using combination of ionic liquids and microwave irradiation. *Progress in Polymer Science*, 36(12):1754-1765, 2011.

[24] Marrucho, I. M., Branco, L. C., and Rebelo, L. P. N. Ionic liquids in pharmaceutical applications. *Annual Review of Chemical and Biomolecular Engineering*, *5*:527-546, 2014.

[25] Sarma, P., Dutta, A. K., and Borah, R. Design and Exploration of $–SO_3H$ Group Functionalized Brønsted Acidic Ionic Liquids (BAILs) as Task-Specific Catalytic Systems for Organic Reactions: A Review of Literature. *Catalysis Surveys from Asia*, 21:70-93, 2017.

[26] Dutta, A. K., Gogoi, P., and Borah, R. Synthesis of dibenzoxanthene and acridine derivatives catalyzed by 1, 3-disulfonic acid imidazolium carboxylate ionic liquids. *RSC advances*, 4(78):41287-41291, 2014.

[27] Amarasekara, A.S. Acidic ionic liquids. *Chemical reviews*, 116(10):6133-6183, 2016.

[28] Wilkes, J. S., Levisky, J. A., Wilson, R. A., and Hussey, C. L. Dialkylimidazolium chloroaluminate melts: a new class of room-temperature ionic liquids for electrochemistry, spectroscopy and synthesis. *Inorganic Chemistry*, 21(3):1263-1264, 1982.

[29] Das, S., Kashyap, N., Kalita, S., Bora, D. B., and Borah, R. A brief insight into the physicochemical properties of room-temperature acidic ionic liquids and their catalytic applications in CC bond formation reactions. In Williams, I. H. and William, N. H., editors, *Advances in Physical Organic Chemistry*, volume 54, pages 1-98, ISBN: 978-0-12-821820-4. Elsevier, London, UK, 2020.

[30] Abbott, A.P., Capper, G., Davies, D.L., Rasheed, R.K., and Tambyrajah, V. Quaternary ammonium zinc-or tin-containing ionic liquids: water insensitive, recyclable catalysts for Diels–Alder reactions. *Green Chemistry*, 4(1):24-26, 2002.

[31] Gilmore, B.F., Andrews, G.P., Borberly, G., Earle, M.J., Gilea, M.A., Gorman, S.P., Lowry, A.F., McLaughlin, M., and Seddon, K.R. Enhanced antimicrobial activities of 1-alkyl-3-methyl imidazolium ionic liquids based on silver or copper containing anions. *New journal of chemistry*, 37(4):873-876, 2013.

[32] Estager, J., Holbrey, J.D., and Swadźba-Kwaśny, M. Halometallate ionic liquids–revisited. *Chemical Society Reviews*, 43(3):847-886, 2014.

[33] Kalita, S., Kashyap, N., Bora, D. B., Das, S., and Borah, R. Investigation of N, N′-Disulfopiperazinium Chlorometallates of Fe (III), Ni (II) and Co (II) as Hybrid Catalysts for the Synthesis of 1, 2-Dihydroquinazoline Derivatives. *ChemistrySelect*, 8(18):e202204533, 2023.

[34] Dutta, A. K., Gogoi, P., and Borah, R. Diethyldisulfoammonium chlorometallates as heterogeneous Brønsted–Lewis acidic catalysts for one-pot synthesis of 14-aryl-7-(N-phenyl)-14H-dibenzo [a, j] acridines. *Applied Organometallic Chemistry*, 32(1):e3900, 2018.

[35] Saikia, S., Puri, K., and Borah, R. Supported dual-acidic 1, 3-disulfoimidazolium chlorozincate@ HZSM-5 as a promising heterogeneous catalyst for synthesis of indole derivatives. *Applied Organometallic Chemistry*, 33(3):e4672, 2019.

[36] Wu, T.Y., Su, S.G., Lin, Y.C., Wang, H.P., Lin, M.W., Gung, S.T., and Sun, I.W. Electrochemical and physicochemical properties of cyclic amine-based Brønsted acidic ionic liquids. *Electrochimica Acta*, *56*(2):853-862, 2010.

[37] Chiappe, C. and Rajamani, S. Structural effects on the physico-chemical and catalytic properties of acidic ionic liquids: an overview. *European Journal of Organic Chemistry*, 2011(28):5517-5539, 2011.

[38] Fernandes, A. M., Rocha, M. A., Freire, M.G., Marrucho, I. M., Coutinho, J. A., and Santos, L. M., 2011. Evaluation of cation− anion interaction strength in ionic liquids. *The Journal of Physical Chemistry B*, *115*(14):4033-4041, 2011.

[39] Yuan, W.L., Yang, X., He, L., Xue, Y., Qin, S., and Tao, G.H. Viscosity, conductivity, and electrochemical property of dicyanamide ionic liquids. *Frontiers in Chemistry*, *6*:59, 2018.

[40] Pinkert, A., Ang, K.L., Marsh, K.N., and Pang, S. Density, viscosity and electrical conductivity of protic alkanolammonium ionic liquids. *Physical Chemistry Chemical Physics*, 13(11):5136-5143, 2011.

[41] Wu, F., Xiang, J., Chen, R., Li, L., Chen, J. and Chen, S. The structure− activity relationship and physicochemical properties of acetamide-based Brønsted acid ionic liquids. *The Journal of Physical Chemistry C*, 114(47):20007-20015, 2010.

[42] Zhou, H., Chen, L., Wei, Z., Lu, Y., Peng, C., Zhang, B., Zhao, X., Wu, L., and Wang, Y. Effect of ionic composition on physicochemical properties of mono-ether functional ionic liquids. *Molecules*, 24(17):3112, 2019.

[43] Thawarkar, S., Khupse, N. D., and Kumar, A. Comparative investigation of the ionicity of aprotic and protic ionic liquids in molecular solvents by using conductometry and NMR spectroscopy. *ChemPhysChem*, 17(7):1006-1017, 2016.

[44] Anouti, M., Couadou, E., Timperman, L., and Galiano, H. Protic ionic liquid as electrolyte for high-densities electrochemical double layer capacitors with activated carbon electrode material. *Electrochimica Acta*, 64:110-117, 2012.

[45] Thawarkar S, Khupse, N. D., and Kumar, A. Solvent-mediated molar conductivity of protic ionic liquids. *Physical Chemistry Chemical Physics*, 17(1):475-482, 2015.

[46] Amarasekara, A.S. and Owereh, O.S. Thermal properties of sulfonic acid group functionalized Brönsted acidic ionic liquids. *Journal of thermal analysis and calorimetry*, *103*(3):1027-1030, 2011.

[47] Pebdani, Z. H., Hajipour, A. R., and Ghayeba, Y. Thermo physical properties of Lewis acidic ionic liquids [Bu_3NBn] Cl-2(MCl_m), (MCl_m = $AlCl_3$, $FeCl_3$, $CuCl_2$, $SnCl_4$, $ZnCl_2$) binary mixtures with DMSO at Temperatures from (298.15 to 363.15) K. *International Journal of Analysis in Medicinal Chemistry,* 2:1–12, 2019.

[48] O'Mahony, A.M., Silvester, D.S., Aldous, L., Hardacre, C., and Compton, R.G. Effect of water on the electrochemical window and potential limits of room-

temperature ionic liquids. *Journal of Chemical & Engineering Data*, 53(12):2884-2891, 2008.

[49] Stettner, T., Gehrke, S., Ray, P., Kirchner, B., and Balducci, A. Water in Protic Ionic Liquids: Properties and Use of a New Class of Electrolytes for Energy-Storage Devices. *ChemSusChem*, *12*(16):3827-3836, 2019.

[50] Shmukler, L. E., Gruzdev, M. S., Kudryakova, N. O., Fadeeva, Y. A., Kolker, A. M. and Safonova, L. P. Thermal behavior and electrochemistry of protic ionic liquids based on triethylamine with different acids. *RSC advances*, 6(111):109664-109671, 2016.

[51] Thomazeau, C., Olivier-Bourbigou, H., Magna, L., Luts, S. and Gilbert, B. Determination of an acidic scale in room temperature ionic liquids. *Journal of the American Chemical Society*, 125(18):5264-5265, 2003.

[52] Gräsvik, J., Hallett, J.P., To, T.Q., and Welton, T. A quick, simple, robust method to measure the acidity of ionic liquids. *Chemical Communications*, *50*(55):7258-7261, 2014.

[53] Estager, J., Oliferenko, A.A., Seddon, K.R., and Swadźba-Kwaśny, M., Chlorometallate (iii) ionic liquids as Lewis acidic catalysts–a quantitative study of acceptor properties. *Dalton Transactions*, 39(47):11375-11382, 2010.

[54] Duan, Z., Gu, Y., and Deng, Y. Green and moisture-stable Lewis acidic ionic liquids (choline chloride· xZnCl2) catalyzed protection of carbonyls at room temperature under solvent-free conditions. *Catalysis Communications*, *7*(9):651-656, 2006.

[55] Yim, T., Choi, C.Y., Mun, J., Oh, S.M., and Kim, Y.G. Synthesis and properties of acyclic ammonium-based ionic liquids with allyl substituents as electrolytes. *Molecules*, 14(5):1840-1851, 2009.

[56] Zhou, Z.B., Matsumoto, H., and Tatsumi, K., Low-melting, low-viscous, hydrophobic ionic liquids: aliphatic quaternary ammonium salts with perfluoroalkyltrifluoroborates. *Chemistry–A European Journal*, 11(2):752-766, 2005.

[57] Keshapolla, D., Srinivasarao, K. and Gardas, R.L. Influence of temperature and alkyl chain length on physicochemical properties of trihexyl-and trioctylammonium based protic ionic liquids. *The Journal of Chemical Thermodynamics*, 133:170-180, 2019.

[58] Greaves, T.L., Weerawardena, A., Fong, C., Krodkiewska, I., and Drummond, C.J. Protic ionic liquids: solvents with tunable phase behavior and physicochemical properties. *The Journal of Physical Chemistry B*, 110(45):22479-22487, 2006.

[59] Hanabusa, H., Takeoka, Y., Rikukawa, M., and Yoshizawa-Fujita, M. Effect of alkyl chain length in anions on the physicochemical properties of cellulose-dissolving protic ionic liquids. *Australian Journal of Chemistry*, 72(2):55-60, 2018.

[60] Zheng, Y., Dong, K., Wang, Q., Zhang, J., and Lu, X. Density, viscosity, and conductivity of Lewis acidic 1-butyl-and 1-hydrogen-3-methylimidazolium chloroaluminate ionic liquids. *Journal of Chemical & Engineering Data*, 58(1):32-42, 2013.

[61] Ullah, Z., Bustam, M.A., Man, Z., Muhammad, N., and Khan, A.S. Synthesis, characterization and the effect of temperature on different physicochemical properties of protic ionic liquids. *RSC advances*, 5(87):71449-71461, 2015.

[62] Bhattacharjee, A., Coutinho, J.A., Freire, M.G., and Carvalho, P.J. Thermophysical properties of two ammonium-based protic ionic liquids. *Journal of Solution Chemistry*, 44:703-717, 2015.

[63] Ullah, Z., Bustam, M.A., Man, Z., Shah, S.N., Khan, A.S., and Muhammad, N. 2016. Synthesis, characterization and physicochemical properties of dual-functional acidic ionic liquids. *Journal of Molecular Liquids*, 223:81-88, 2016.

[64] Dorbritz, S., Ruth, W., and Kragl, U. Investigation on aggregate formation of ionic liquids. *Advanced Synthesis & Catalysis*, 347(9):1273-1279, 2005.

[65] Boruń, A. and Bald, A. Ionic association and conductance of ionic liquids in dichloromethane at temperatures from 278.15 to 303.15 K. *Ionics*, 22:859-867, 2016.

[66] Canongia Lopes, J. N., Costa Gomes, M. F., and Pádua, A. A. Nonpolar, polar, and associating solutes in ionic liquids. *The Journal of Physical Chemistry B*, 110(34):16816-16818, 2006.

[67] Wang, Y. and Voth, G. A. Unique spatial heterogeneity in ionic liquids. *Journal of the American Chemical Society*, 127(35):12192-12193, 2005.

[68] Bowers, J., Butts, C. P., Martin, P. J., Vergara-Gutierrez, M. C., and Heenan, R. K. Aggregation behavior of aqueous solutions of ionic liquids. *Langmuir*, 20(6):2191-2198, 2004.

[69] Xu, L., Cui, X., Zhang, Y., Feng, T., Lin, R., Li, X., and Jie, H. Measurement and correlation of electrical conductivity of ionic liquid [EMIM][DCA] in propylene carbonate and γ-butyrolactone. *Electrochimica Acta*, 174:900-907, 2015.

[70] Wang, J., Greaves, T. L., Kennedy, D. F., Weerawardena, A., Song, G., and Drummond, C.J. Amino acid-derived protic ionic liquids: physicochemical properties and behaviour as amphiphile self-assembly media. *Australian Journal of Chemistry*, 64(2):180-189, 2011.

[71] Srinivasa Rao, K., Singh, T., Trivedi, T.J. and Kumar, A. Aggregation behavior of amino acid ionic liquid surfactants in aqueous media. *The Journal of Physical Chemistry B*, 115(47):13847-13853, 2011.

[72] Yang, X. J., Zhang, P., Lv, W., Zhou, T., Li, P., and Zhao, M. Aggregation Behavior of Imidazolium-Based Amino Acid Ionic Liquid Surfactants in Aqueous Solution: The Effect of Amino Acid Counterions. *Journal of Surfactants and Detergents*, 22(3):515-523, 2019.

[73] Saikia, S., Gogoi, P., Dutta, A. K., Sarma, P., and Borah, R. Design of multifaceted acidic 1, 3-disulfoimidazolium chlorometallate ionic systems as heterogeneous catalysts for the preparation of β-amino carbonyl compounds. *Journal of Molecular Catalysis A: Chemical*, 416:63-72, 2016.

[74] Brzęczek-Szafran, A., Erfurt, K., Swadźba-Kwaśny, M., Piotrowski, T., and Chrobok, A. Beckmann Rearrangement with Improved Atom Economy, Catalyzed by Inexpensive, Reusable, Brønsted Acidic Ionic Liquid. *ACS Sustainable Chemistry & Engineering*, 10(41):13568-13575, 2022.

[75] Gogoi, P., Dutta, A. K., Sarma, P., and Borah, R. Development of Brönsted–Lewis acidic solid catalytic system of 3-methyl-1-sulfonic acid imidazolium transition metal chlorides for the preparation of bis (indolyl) methanes. *Applied Catalysis A: General*, 492:133-139, 2015.

[76] Lyu, X., Wang, W., Sun, Y., Zhao, Q., and Qiu, T. Ionic Liquids Catalyzed Friedel–Crafts Alkylation of Substituted Benzenes with CCl_4 Toward Trichloromethylarenes. *Catalysis Letters*, 149:665-671, 2019.

[77] Hajipour, A.R., Ghayeb, Y., Sheikhan, N., and Ruoho, A.E. Brønsted acidic ionic liquid as an efficient and reusable catalyst for one-pot synthesis of 1-amidoalkyl 2-naphthols under solvent-free conditions. *Tetrahedron Letters*, 50(40):5649-5651, 2009.

[78] Wu, Y., Hao, X., Yang, J., Tian, F., and Jiang, M. Ultrasound-assisted synthesis of nanocrystalline ZnS in the ionic liquid [BMIM]·BF_4. *Materials Letters*, 60(21-22):2764-2766, 2006.

[79] Arora, K., Shikha, P., Abdelbaky, R. M. K., and Kang, T. S. Modulation of morphological, optical and magnetic properties of Cr-doped $La_{0.9}Ce_{0.1}$ FeO_3 nanoferrites synthesized by surface-active ionic liquid aided hydrothermal route. *Applied Physics A*, 127:1-9, 2021.

[80] Shikha, P., Kang, T. S., and Randhawa, B. S. Mn doping induced physico-chemical changes in LaCe ferrite nanofabricated by ionic liquid assisted hydrothermal route. *Journal of Alloys and Compounds*, 701:788-796, 2017.

[81] Sekhar, M. C., Santhosh, K., Praveen Kumar, J., Mondal, N., Soumya, S., and Samanta, A. Cdte quantum dots in ionic liquid: stability and hole scavenging in the presence of a sulfide salt. *The Journal of Physical Chemistry C*, 118 (32):18481–18487, 2014

[82] Wang, L., Xu, S. Z., Li, H. J., Chang, L. X., Zeng, M. H., Wang, L. N., and Huang, Y.N. Microbundles of zinc oxide nanorods: Assembly in ionic liquid [EMIM]+[BF4]−, photoluminescence and photocatalytic properties. *Journal of Solid State Chemistry*, 184(3):720-724, 2011.

[83] Alayoglu, S., Nilekar, A. U., Mavrikakis, M., and Eichhorn, B. Ru–Pt core–shell nanoparticles for preferential oxidation of carbon monoxide in hydrogen. *Nature materials*, 7(4):333-338, 2008.

[84] Narayanan, R. and El-Sayed, M. A. Catalysis with transition metal nanoparticles in colloidal solution: nanoparticle shape dependence and stability. *The Journal of Physical Chemistry B*, 109(26):12663-12676, 2005.

[85] Cheng, F., Liang, J., Tao, Z., and Chen, J. Functional materials for rechargeable batteries. *Advanced materials*, 23(15):1695-1715, 2011.

[86] Liu, X.D., Chen, H., Liu, S.S., Ye, L.Q., and Li, Y.P. Hydrothermal synthesis of superparamagnetic Fe_3O_4 nanoparticles with ionic liquids as stabilizer. *Materials Research Bulletin*, 62:217-221, 2015.

[87] Xu, L., Xia, J., Wang, L., Qian, J., Li, H., Wang, K., Sun, K., and He, M. α-Fe_2O_3 Cubes with High Visible-Light-Activated Photoelectrochemical Activity towards Glucose: Hydrothermal Synthesis Assisted by a Hydrophobic Ionic Liquid. *Chemistry–A European Journal*, 20(8): 2244-2253, 2014.

[88] Wang, L., Chang, L.X., Wei, L.Q., Xu, S.Z., Zeng, M.H., and Pan, S.L.The effect of 1-N-alkyl chain of ionic liquids $[C_n$mim]+ Br−(n= 2, 4, 6, 8) on the aspect ratio of ZnO nanorods: syntheses, morphology, forming mechanism, photoluminescence and recyclable photocatalytic activity. *Journal of Materials Chemistry*, 21(39):15732-15740, 2011.

[89] Goharshadi, E.K., Sajjadi, S.H., Mehrkhah, R., and Nancarrow, P. Sonochemical synthesis and measurement of optical properties of zinc sulfide quantum dots. *Chemical Engineering Journal*, 209:113-117, 2012.

[90] Xu, L., Xia, J., Wang, L., Qian, J., Li, H., Wang, K., Sun, K., and He, M. α-Fe_2O_3 Cubes with High Visible-Light-Activated Photoelectrochemical Activity towards Glucose: Hydrothermal Synthesis Assisted by a Hydrophobic Ionic Liquid. *Chemistry–A European Journal*, 20(8): 2244-2253, 2014.

[91] Iida, M., Baba, C., Inoue, M., Yoshida, H., Taguchi, E., and Furusho, H. Ionic liquids of bis (alkylethylenediamine) silver (I) salts and the formation of silver (0) nanoparticles from the ionic liquid system. *Chemistry–A European Journal*, 14(16):5047-5056, 2008.

[92] Liu, X., Ma, J., Peng, P., and Zheng, W. One-pot hydrothermal synthesis of ZnSe hollow nanospheres from an ionic liquid precursor. *Langmuir*, 26(12):9968-9973, 2010.

[93] Zhang, J., Feng, H., Yang, J., Qin, Q., Fan, H., Wei, C., and Zheng, W., 2015. Solvothermal synthesis of three-dimensional hierarchical CuS microspheres from a Cu-based ionic liquid precursor for high-performance asymmetric supercapacitors. *ACS applied materials & interfaces*, 7(39):21735-21744, 2010.

[94] Singh, P., Anand, A., and Kumar, V. Recent developments in biological activities of chalcones: A mini review. *European journal of medicinal chemistry*, 85:758-777, 2014.

[95] Rojas, J., Domínguez, J. N., Charris, J. E., Lobo, G., Payá, M., and Ferrándiz, M. L. Synthesis and inhibitory activity of dimethylamino-chalcone derivatives on the induction of nitric oxide synthase. *European Journal of Medicinal Chemistry*, 37(8):699-705, 2002.

[96] Kidwai, M., Sapra, P., Misra, P., Saxena, R.K., and Singh, M. Microwave assisted solid support synthesis of novel 1, 2, 4-triazolo [3, 4-b]-1, 3, 4-thiadiazepines as

potent antimicrobial agents. *Bioorganic & medicinal chemistry*, 9(2):217-220, 2001.

[97] Pizzuti, L., Martins, P.L., Ribeiro, B.A., Quina, F.H., Pinto, E., Flores, A.F., Venzke, D., and Pereira, C.M. Efficient sonochemical synthesis of novel 3, 5-diaryl-4, 5-dihydro-1H-pyrazole-1-carboximidamides. *Ultrasonics Sonochemistry*, *17*(1):34-37, 2010.

[98] Martins, M.A., Pereira, C.M., Cunico, W., Moura, S., Rosa, F.A., Peres, R.L., Machado, P., Zanatta, N., and Bonacorso, H.G. Ultrasound promoted synthesis of 5-hydroxy-5-trihalomethyl-4, 5-dihydroisoxazoles and β-enamino trihalomethyl ketones in water. *Ultrasonics sonochemistry*, 13(4):364-370, 2006.

[99] Venzke, D., Flores, A.F., Quina, F.H., Pizzuti, L., and Pereira, C.M. Ultrasound promoted greener synthesis of 2-(3, 5-diaryl-4, 5-dihydro-1H-pyrazol-1-yl)-4-phenylthiazoles. *Ultrasonics sonochemistry*, 18(1):370-374, 2011.

[100] Pandhurnekar, C. P., Meshram, E. M., Chopde H.N., and Batra, R. J. Synthesis, characterization, and biological activity of 4-(2-hydroxy-5-(aryl-diazenyl) phenyl)-6-(aryl) pyrimidin-2-ols derivatives. *Organic Chemistry International*, 2013:1-10, 2013.

[101] Shen, J., Wang, H., Liu, H., Sun, Y., and Liu, Z. Brønsted acidic ionic liquids as dual catalyst and solvent for environmentally friendly synthesis of chalcone. *Journal of Molecular Catalysis A: Chemical*, 280(1):24-28, 2008.

[102] Dong F., Jian C., Zhenghao F., Kai G., and Zuliang L. Synthesis of chalcones via Claisen–Schmidt condensation reaction catalyzed by acyclic acidic ionic liquids. *Catalysis Communication*, 9:1924–1927, 2008.

[103] Kunde, L. B., Gade, S. M., Kalyani, V. S., and Gupte, S. P. Catalytic synthesis of chalcone and flavanone using Zn–Al hydrotalcite adhere ionic liquid. *Catalysis Communications*, 10(14):1881-1888, 2009.

[104] Sarda, S. R., Jadhav, W. N., Tekale, S. U., Jadhav, G. V., Patil, B. R., Suryawanshi, G. S., and Pawar, R. P. Phosphonium ionic liquid catalyzed an efficient synthesis of chalcones. *Letters in Organic Chemistry*, 6(6):481-484, 2009.

[105] Pan, X., Yi, F., Zhang, X., and Chen, S. Synthesis of amino chalcones in presence of ionic liquid as soluble support. *Asian Journal of Chemistry*, 24(9):3809, 2012.

[106] Qian H., Liu D., and Lv C. Synthesis of chalcones via Claisen-Schmidt reaction catalyzed by sulfonic acid-functional ionic liquids. *Industrial & Engineering Chemistry Research*, 50:1146–1149, 2011.

[107] Davoodnia, A. and Yassaghi, G. Solvent-free selective cross-aldol condensation of ketones with aromatic aldehydes efficiently catalyzed by a reusable supported acidic ionic liquid. *Chinese Journal of Catalysis*, 33(11):1950-1957, 2012.

[108] Qian, H., Wang, Y., and Liu, D. Ultrasound-accelerated synthesis of substituted 2′-hydroxychalcones by reusable ionic liquids. *Industrial & Engineering Chemistry Research*, *52*(37):13272-13275, 2013.

[109] Xiaoyun, H., Liyan, W., Shishi, Z., and Jinsheng, X. A green synthesis of chalcones catalyzed by an alkaline ionic liquid under solvent-free condition. *Journal of South-Central University for Nationalities (Nat.Sci.Edition)*, 34(4):20-23, 2015.

[110] Sharma, V., Kumar, P. and Pathak, D. Biological importance of the indole nucleus in recent years: a comprehensive review. *Journal of Heterocyclic Chemistry*, 47(3): 491-502, 2010.

[111] Zhang, H.B., Liu, L., Liu, Y.L., Chen, Y.J., Wang, J. and Wang, D. Triflic Acid–Catalyzed Michael Reactions of indole and pyrrole compounds with α, β-Unsaturated Ketones in Water. *Synthetic communications*, 37(2): 173-181, 2007.

[112] Srivastava, N. and Banik, B.K. Bismuth nitrate-catalyzed versatile Michael reactions. *The Journal of organic chemistry*, 68(6): 2109-2114, 2003.

[113] Bartoli, G., Bartolacci, M., Bosco, M., Foglia, G., Giuliani, A., Marcantoni, E., Sambri, L. and Torregiani, E. h Michael Addition of Indoles to α, β-Unsaturated Ketones Catalyzed by $CeCl_3$.7H2O− NaI Combination Supported on Silica G l1. *The Journal of organic chemistry*, 68(11): 4594-4597, 2003.

[114] Khabazzadeh, H., Kermany, E.T. and Eghbali, M. $Cs_{2.5}H_{0.5}PW_{12}O_{40}$-catalyzed conjugate addition of indole to α, β-unsaturated ketones. *Arabian Journal of Chemistry*, 9: S659-S662, 2016.

[115] Maiti, G. and Kundu, P. Antimony Trichloride–Catalyzed Michael Addition of indoles to the α,β-Unsaturated Ketones. *Synthetic Communications*, 37(14): .2309-2316, 2007

[116] Yaragorla, S. and Kumar, G.S. A facile method for the synthesis of various 3-substituted indoles via Michael addition reaction using NbCl5. *Indian Journal of Chemistry*, 54(B): 240-244, 2015.

[117] Ekbote, S.S., Panda, A.G., Bhor, M.D., and Bhanage, B.M. Polyvinylsulfonic acid as a novel Brønsted acid catalyst for Michael addition of indoles to α, β-unsaturated ketones. *Catalysis Communications*, 10(12):1569-1573, 2009.

[118] Gu, D.G., Ji, S.J., Wang, H. X., and Xu, Q. Y. Acidic Ionic Liquid–Catalyzed Highly Efficient Reaction of Indoles to α, β-Unsaturated Ketones. *Synthetic Communications*, 38(8):1212-1223, 2008.

[119] Yu, C.J. and Liu, C.J. Conjugate Addition of Indoles to α, β-Unsaturated Ketones Using a Brønsted Acid Ionic Liquid as an Efficient Catalyst. *Molecules*, 14(9):3222-3228, 2009.

[120] Wang, B., and Liu, C. J. Novel Brønsted Acidic Ionic Liquids Based on Benzimidazolium Cation: Synthesis and Catalyzed Conjugate Addition of Indoles with α, β-unsaturated Ketones. *Advanced Materials Research*, 233:977-984, 2011.

[121] Ma, X., Liu, X., and Liu, C. The Michael Addition Reaction of Indoles and α, β-Unsaturated Ketones Catalyzed by Brønsted Acidic Ionic Liquid. *Journal of Organic Chemistry Research*, 5(2):86-93, 2017.

[122] Hagiwara, H., Sekifuji, M., Hoshi, T., Suzuki, T., Quanxi, B., Qiao, K., and Yokoyama, C. Sustainable conjugate addition of indoles catalyzed by acidic ionic liquid immobilized on silica. *Synlett*, 2008(04):608-610, 2008.

[123] Yadav, J. S., Reddy, B. V. S., Baishya, G., Reddy, K. V., and Narsaiah, A. V. Conjugate addition of indoles to α, β-unsaturated ketones using Cu (OTf) 2 immobilized in ionic liquids. *Tetrahedron*, 61(40):9541-9544, 2005.

[124] Li, W. J., Lin, X. F., Wang, J., Li, G. L., and Wang, Y. G. Palladium-catalyzed michael addition of indoles to α, β-unsaturated ketones in an ionic liquid. *Synlett*, 2005(13):2003-2006, 2005.

[125] Mamedov, I., Naghiyev, F., Maharramov, A., Uwangue, O., Farewell, A., Sunnerhagen, P., and Erdelyi, M. Antibacterial activity of 2-amino-3-cyanopyridine derivatives. *Mendeleev Communications*, 30(4):498-499, 2020.

[126] Mantri, M., de Graaf, O., van Veldhoven, J., Göblyös, A., von Frijtag Drabbe Künzel, J.K., Mulder-Krieger, T., Link, R., de Vries, H., Beukers, M. W., Brussee, J., and IJzerman, A.P., 2008. 2-Amino-6-furan-2-yl-4-substituted nicotinonitriles

as A2A adenosine receptor antagonists. *Journal of Medicinal Chemistry*, 51(15):4449-4455, 2008

[127] Murata, T., Shimada, M., Sakakibara, S., Yoshino, T., Masuda, T., Shintani, T., Sato, H., Koriyama, Y., Fukushima, K., Nunami, N., and Yamauchi, M. Synthesis and structure–activity relationships of novel IKK-β inhibitors. Part 3: Orally active anti-inflammatory agents. *Bioorganic & Medicinal Chemistry Letters*, 14(15):4019-4022, 2004.

[128] Ayvaz, S., Çankaya, M., Atasever, A., and Altuntas, A. 2-Amino-3-cyanopyridine derivatives as carbonic anhydrase inhibitors. *Journal of Enzyme Inhibition and Medicinal Chemistry*, 28(2): 305-310, 2013.

[129] Deng, J., Sanchez, T., Al-Mawsawi, L.Q., Dayam, R., Yunes, R.A., Garofalo, A., Bolger, M.B. and Neamati, N. Discovery of structurally diverse HIV-1 integrase inhibitors based on a chalcone pharmacophore. *Bioorganic & Medicinal Chemistry*, *15*(14):4985-5002, 2007.

[130] Thakrar, S., Bavishi, A., Radadiya, A., Vala, H., Parekh, S., Bhavsar, D., Chaniyara, R., and Shah, A. An Efficient microwave-assisted synthesis and antimicrobial activity of novel 2-amino 3-cyano pyridine derivatives using two reusable solid acids as catalysts. *Journal of Heterocyclic chemistry*, 51(3):555-561, 2014.

[131] Lang, D. K., Kaur, R., Arora, R., Saini, B. and Arora, S. Nitrogen-containing heterocycles as anticancer agents: An overview. *Anti-Cancer Agents in Medicinal Chemistry (Formerly Current Medicinal Chemistry-Anti-Cancer Agents)*, 20(18):2150-2168, 2020.

[132] Sarda, S.R., Kale, J.D., Wasmatkar, S.K., Kadam, V.S., Ingole, P.G., Jadhav, W.N., and Pawar, R.P. An efficient protocol for the synthesis of 2-amino-4, 6-diphenylpyridine-3-carbonitrile using ionic liquid ethylammonium nitrate. *Molecular Diversity*, 13(4):545-549, 2009.

[133] Wan, Y., Yuan, R., Zhang, F.R., Pang, L. L., Ma, R., Yue, C. H., Lin, W., Yin, W., Bo, R.C., and Wu, H. One-pot synthesis of N2-substituted 2-amino-4-aryl-5, 6, 7, 8-tetrahydroquinoline-3-carbonitrile in basic ionic liquid [bmim] OH. *Synthetic Communications*, 41(20):2997-3015, 2011.

[134] Mansoor, S.S., Aswin, K., Logaiya, K., and Sudhan, S.P.N. [Bmim] BF4 ionic liquid: An efficient reaction medium for the one-pot multi-component synthesis of

2-amino-4, 6-diphenylpyridine-3-carbonitrile derivatives. *Journal of Saudi Chemical Society*, 20(5):517-522, 2016.

[135] Tamaddon, F. and Azadi, D. Nicotinium methane sulfonate (NMS): A bio-renewable protic ionic liquid and bi-functional catalyst for synthesis of 2-amino-3-cyano pyridines. *Journal of Molecular Liquids*, 249:789-794, 2018.

[136] Mollashahi, E. and Bazgiri, A. Acidic Brønsted ionic liquids catalyzed the preparation of 2-amino-3-cyanopyridine derivatives under ambient and solvent-free conditions. *Applied Chemistry*, 12(45):11-20, (2017).

[137] Jalali-Mola, S., Torabi, M., Yarie, M., and Zolfigol, M. A. Acidic tributyl phosphonium-based ionic liquid: an efficient catalyst for preparation of diverse pyridine systems via a cooperative vinylogous anomeric-based oxidation. *RSC Advances*, 12(53):34730-34739, 2022.

[138] He, Z. and Alexandridis, P. Nanoparticles in Ionic Liquids: Interactions and Organization. *Physical Chemistry Chemical Physics*, 17 (28):18238–18261, 2015.

[139] Wegner, S. and Janiak, C. Metal nanoparticles in ionic liquids. *Topics in Current Chemistry*, 375:1-32, 2017.

[140] Fu, Q. and Wagner, T. Interaction of nanostructured metal overlayers with oxide surfaces. *Surface Science Reports*, 62(11):431-498, 2007.

[141] Henrist, C., Mathieu, J.P., Vogels, C., Rulmont, A., and Cloots, R. Morphological study of magnesium hydroxide nanoparticles precipitated in dilute aqueous solution. *Journal of Crystal Growth*, 249(1-2):321-330, 2003.

[142] Shikha, P., Kang, T. S., and Randhawa, B. S. Ionic liquid assisted nanofabrication of ferromagnetic Co-doped La–Ce ferrites. *RSC advances*, 5(117):96799-96808, 2015.

[143] Wender, H., Andreazza, M. L., Correia, R. R., Teixeira, S. R., and Dupont, J. Synthesis of gold nanoparticles by laser ablation of an Au foil inside and outside ionic liquids. *Nanoscale*, 3(3):1240-1245, 2011.

[144] Arora, K., Singh, G., Karthikeyan, S., and Kang, T. S. One-pot sustainable preparation of sunlight active ZnS@ graphene nano-composites using a Zn containing surface active ionic liquid. *Nanoscale Advances*, 2(10):4770-4776, 2020.